OPEN ACCESS

EXTENDED REPORT

HRES-1/Rab4-mediated depletion of Drp1 impairs mitochondrial homeostasis and represents a target for treatment in SLE

Tiffany N Caza,[1] David R Fernandez,[1] Gergely Talaber,[1] Zachary Oaks,[1] Mark Haas,[2] Michael P Madaio,[3] Zhi-wei Lai,[1] Gabriella Miklossy,[1] Ram R Singh,[4] Dmitriy M Chudakov,[5] Walter Malorni,[6] Frank Middleton,[1] Katalin Banki,[1] Andras Perl[1]

Handling editor Tore K Kvien

▶ Additional material is published online only. To view please visit the journal online (http://dx.doi.org/10.1136/annrheumdis-2013-203794).

For numbered affiliations see end of article

Correspondence to Dr Andras Perl, Department of Medicine, State University of New York, 750 East Adams Street, Syracuse, New York 13210, USA; perla@upstate.edu

Received 16 April 2013
Revised 13 June 2013
Accepted 9 July 2013
Published Online First 29 July 2013

To cite: Caza TN, Fernandez DR, Talaber G, *et al*. *Ann Rheum Dis* 2014;**73**:1888–1897.

ABSTRACT

Objective Accumulation of mitochondria underlies T-cell dysfunction in systemic lupus erythematosus (SLE). Mitochondrial turnover involves endosomal traffic regulated by HRES-1/Rab4, a small GTPase that is overexpressed in lupus T cells. Therefore, we investigated whether (1) HRES-1/Rab4 impacts mitochondrial homeostasis and (2) Rab geranylgeranyl transferase inhibitor 3-PEHPC blocks mitochondrial accumulation in T cells, autoimmunity and disease development in lupus-prone mice.

Methods Mitochondria were evaluated in peripheral blood lymphocytes (PBL) of 38 SLE patients and 21 healthy controls and mouse models by flow cytometry, microscopy and western blot. MRL/lpr mice were treated with 125 μg/kg 3-PEHPC or 1 mg/kg rapamycin for 10 weeks, from 4 weeks of age. Disease was monitored by antinuclear antibody (ANA) production, proteinuria, and renal histology.

Results Overexpression of HRES-1/Rab4 increased the mitochondrial mass of PBL (1.4-fold; p=0.019) and Jurkat cells (2-fold; p=0.000016) and depleted the mitophagy initiator protein Drp1 both in human (−49%; p=0.01) and mouse lymphocytes (−41%; p=0.03). Drp1 protein levels were profoundly diminished in PBL of SLE patients (−86±3%; p=0.012). T cells of 4-week-old MRL/lpr mice exhibited 4.7-fold over-expression of Rab4A (p=0.0002), the murine homologue of HRES-1/Rab4, and depletion of Drp1 that preceded the accumulation of mitochondria, ANA production and nephritis. 3-PEHPC increased Drp1 (p=0.03) and reduced mitochondrial mass in T cells (p=0.02) and diminished ANA production (p=0.021), proteinuria (p=0.00004), and nephritis scores of lupus-prone mice (p<0.001).

Conclusions These data reveal a pathogenic role for HRES-1/Rab4-mediated Drp1 depletion and identify endocytic control of mitophagy as a treatment target in SLE.

INTRODUCTION

Mitochondrial dysfunction, characterised by the persistent elevation of the mitochondrial transmembrane potential ($\Delta\Psi_m$) or mitochondrial hyperpolarisation (MHP), oxidative stress and depletion of intracellular adenosine triphosphate (ATP) and glutathione, plays fundamental roles in abnormal T-cell activation in patients with SLE.[1–3] The mammalian target of rapamycin (mTOR) serves as a sensor of mitochondrial homeostasis in T cells[4] and is activated in SLE patients.[5] Blockade of mTOR with rapamycin improved disease activity in murine lupus[6] and in SLE patients.[7] N-acetylcysteine (NAC), which serves as both a precursor of glutathione and antioxidant in and of itself, also diminished disease activity in SLE patients, through inhibiting mTOR.[8] However, mTOR blockade with either rapamycin[7] or NAC failed to reverse MHP and the accumulation of mitochondria,[8] indicating that mitochondrial dysfunction is located upstream of mTOR activation in SLE.

The efficacy of mTOR blockade is related to the reversal of enhanced Ca^{2+} signalling through the T-cell receptor,[7] which is attributed to the lysosomal degradation of CD4 and CD3ζ[5] and their substitution by FcεRIγ[9] which, in turn, are regulated by the small GTPase HRES-1/Rab4 through endosomal traffic.[5] mTOR has been localised to endosomes,[10] including those carrying HRES-1/Rab4.[5] Polymorphic alleles of HRES-1 locus are associated with SLE[11 12] and influence expression of HRES-1/Rab4,[13] which may represent the gene product that confers susceptibility to lupus at 1q42.[14] Although mTOR has been widely implicated in the suppression of autophagy,[15 16] the opposing effects of rapamycin on the degradation of proteins, such as CD4 and CD3ζ, and organelles, such as mitochondria, both of which occur in lysosomes, appear paradoxical. During autophagy, proteins and organelles alike are carried to the lysosome as endosomal cargo.[17] Therefore, we examined the role of HRES-1/Rab4, which is overexpressed in T cells of SLE patients,[5] as a selective regulator of autophagy pathways, that is, facilitator of protein microautophagy and inhibitor of organelle macroautophagy.

Autophagy is a fundamental stress-induced catabolic process that moves cargo to the lysosome through three main mechanisms: (1) microautophagy, transferring cytoplasmic materials into the lysosome though endosome fusion, (2) chaperone-mediated autophagy that requires binding of a chaperone first to its cytosolic protein target and second to a receptor on the lysosomal membrane followed by translocation of the cytosolic protein

into the lysosome and (3) macroautophagy, characterised by the formation of a cytosolic double-membrane vesicle primarily involving organelles such as mitochondria.[18] Macroautophagy of mitochondria or mitophagy is initiated by the translocation of dynamin-related protein 1 (Drp1) from the cytosol to mitochondria, which causes the fission, fragmentation and lysosomal degradation of mitochondria.[17 19] Here, we reveal that HRES-1/Rab4 promotes the lysosomal degradation of Drp1 in Jurkat human T cells. The overexpression of HRES-1/Rab4 increased mitochondrial mass in Jurkat cells and PBL. Drp1 was reduced in lupus T cells and was unaffected by mTOR blockade, similar to the persistence of mitochondrial accumulation in rapamycin-treated patients. Moreover, expression of the murine homologue of HRES-1/Rab4, Rab4A, was found to be increased, while Drp1 was found to be decreased in the spleen and thymus of lupus-prone NZB/W F1 and MRL/lpr mice relative to C57BL/6 controls at 4 weeks of age well before the onset of ANA production, proteinuria and glomerulonephritis (GN). Treatment with Rab geranylgeranyl transferase inhibitor 3-PEHPC, which inactivated HRES-1/Rab4, reversed the depletion of Drp1 as well as the accumulation of mitochondria, and prevented ANA production and nephritis in MRL/lpr mice.

MATERIALS AND METHODS

Human subjects

Thirty-eight patients with SLE were investigated; each patient satisfied the criteria for a definitive diagnosis.[20 21] As controls, 21 healthy subjects were matched for gender, ethnicity and age within 10 years of SLE patients for each blood donation and studied in parallel. Additional details are provided in the online supplementary methods section.

Separation and culture of human PBL

Peripheral blood mononuclear cells (PBMC) were isolated from heparinised venous blood on Ficoll–Hypaque gradient. Peripheral blood lymphocytes (PBL) were separated from monocytes by adherence to autologous serum-coated Petri dishes.[22] T cells (>95% CD3) were negatively isolated from PBMC with Dynal magnetic beads conjugated to IgG antibodies for CD14, CD16 human leukocyte antigen (HLA) class II DR/DP, CD56 and CD235a; Invitrogen Cat No 113-11D). CD4 T cells (>98% CD4) were negatively isolated with magnetic beads conjugated to IgG antibodies for CD8, CD14, CD16, HLA class II DR/DP, CD56, CDw123 and CD235a (Invitrogen Cat No 113-39D). The resultant cell population was resuspended at 10^6 cells/mL in RPMI 1640 medium, supplemented with 10% fetal calf serum (FCS), 2 mM L-glutamine, 100 IU/mL penicillin, and 100 μg/mL gentamicin in 12-well plates at 37°C in a humidified atmosphere with 5% CO_2. Cross-linking of the CD3 antigen was performed by addition of cells to plates precoated with 1 μg/mL OKT3 monoclonal antibody (CRL 8001 from ATCC, Rockville, MD) for 1 h at 37°C. CD28 costimulation was performed with 500 ng/mL mAb CD28.2 (Pharmingen, San Diego, California).

Mice

Female New Zealand White (NZW), NZW×New Zealand Black F1 (NZB/W F1), B6.NZMSle1/Sle2/Sle3, MRL, MRL/lpr, C57BL/6 (B6), and C57BL/6.Lpr (B6/Lpr) mice were obtained from Jackson laboratories (Bar Harbor, ME). Additional details are provided in the online supplementary methods section.

Mouse embryonic fibroblasts (MEFs)

MEFs deficient in Drp1[23] and control MEFs were cultured in DMEM medium supplemented with 10% FBS, 2 mM L-glutamine, 100 U/mL penicillin, 100 μg/mL streptomycin, 10 μg/mL amphotericin B, 1% MEM non-essential amino acid solution (10 mM, Invitrogen), and 1 mM sodium pyruvate.[23]

Flow cytometric analysis of $\Delta\Psi_m$, mitochondrial mass and nitric oxide

Flow cytometry was performed on freshly isolated cells, as described in the online supplementary methods section.

Microarray analysis of gene expression

Biotinylated cRNA was produced by in vitro transcription and hybridised to Affymetrix HG-U133 Plus-2 chips, as described in the online supplementary methods section.

Western blot analysis

Protein lysates were separated by SDS-PAGE, transferred to nitrocellulose, probed with antibodies, and analysed, as described in the online supplementary methods section.

Transfection of siRNA

Knock-down of HRES-1/Rab4 via siRNA transfection is described in the online supplementary methods section.

Transduction of HRES-1/Rab4 by adeno-associated virus

HRES-1/Rab4 cDNA was cloned upstream of the internal ribosomal entry site (IRES) in pAAV-IRES-GFP vector, as described in the online supplementary methods section.

Confocal microscopy

Lysosomal compartments were labelled LysoTracker Red (LTR). Mitochondria were visualised by staining with MitoTracker Deep Red (MTDR). Additional details are provided in the online supplementary methods section.

Autophagy induction

Autophagy was induced with 50 nM rapamycin in the presence and absence of lysosomal inhibitor, 200 nM bafilomycin A1, as described in the online supplementary methods section.

In vitro prenylation assay

Prenylation of HRES-1/Rab4 and Rab5 was evaluated by western blot of soluble and insoluble fractions from Triton×114-treated Jurkat cells, as described in the online supplementary methods section.

Treatment of MRL/lpr mice with Rab geranylgeranyl transferase inhibitor 3-PEHPC and rapamycin

4-week-old MRL/lpr mice were separated into four treatment groups receiving phosphate-buffered saline (PBS) (solvent control for 3-PEHPC; n=4), 125 μg/kg 3-PEHPC in PBS (n=8), 0.2% carboxymethylcellulose (CMC, solvent control for rapamycin, n=4), or 1 mg/kg rapamycin in CMC (n=8). Proteinuria was monitored every 2 weeks between 4–14 weeks of age. To assess treatment toxicity, mice were weighed weekly. Renal pathology was assessed by scoring for glomerulonephritis (GN), glomerulosclerosis (GS), and interstitial nephritis (IN) on a 0–4 scale, and percentage of sclerotic and crescentric glomeruli, as described in the online supplementary methods section.

ANA and cytokine assays

ANA, IFN-γ, IL-10 and IL-17A were measured by ELISA, as described in the online supplementary methods section.

Statistical analyses

Statistical analyses were performed using Statview V.5.0.1 (SAS Institute, Cary, North Carolina) and GraphPad Prism V.5.0 Software (San Diego, California). Additional details are provided in the online supplementary methods section.

Supplementary materials include supplemental methods and online supplementary figures S1–S7.

RESULTS

HRES-1/Rab4 promotes the lysosomal degradation of Drp1

To assess the impact of HRES-1/Rab4 on autophagy pathways, we evaluated global gene expression in Jurkat cells carrying doxycycline-inducible GFP-producing, HRES-1/Rab4 and GFP-producing, or dominant-negative HRES-1/Rab4^{S27N} (HRES-1/Rab4-DN) and GFP-producing expression vector following incubation with or without doxycycline for 24 h[13]; 116 genes exhibited doxycycline-induced reciprocal changes of expression in response to HRES-1/Rab4 relative to HRES-1/Rab4-DN at 99.99% CIs (data not shown). Pathway analysis on the basis of protein–protein interaction with Strings 9.0 software (http://string-db.org) indicated a predominant influence of HRES-1/Rab4 on genes involved in mitochondrial outer membrane organisation (false discovery rate p value with Bonferrroni correction (FRD $p=1.8\times10^{-9}$), membrane raft formation ($p=7.5\times10^{-9}$), and mTOR activation ($p=9.7\times10^{-3}$). The predictive protein interactome analysis implicated genes in addition to the ones revealed by the microarray studies, such as Drp1 and AKAP10. Drp1 initiates the fission and autophagy of mitochondria.[19] In turn, Drp1 is phosphorylated by protein kinase A (PKA)[19] that associates with the endosomal membrane via the PKA anchoring protein AKAP10.[24] As mitochondrial turnover involves endosomal traffic regulated by HRES-1/Rab4, a small GTPase that is overexpressed in lupus T cells, it was important to evaluate the impact of HRES-1/Rab4 on Drp1 and AKAP10.

The functional consequences of HRES-1/Rab4 overexpression on Drp1 were initially evaluated in Jurkat human T cells. As shown in figure 1A, the over-expression of HRES-1/Rab4 reduced Drp1 protein levels by 49% ($p=0.01$). The phosphorylation of Drp1 at Ser 637 was also reduced by HRES-1/Rab4 (66% decrease, $p=0.005$, figure 1A). As Drp1 is phosphorylated at Ser 637 by PKA, which is anchored to endosomes via AKAP10,[24] we also evaluated the effect of HRES-1/Rab4 on AKAP10. As shown in figure 1A, AKAP10 protein levels were reduced by HRES-1/Rab4-DN. Both the HRES-1/Rab4-induced depletion of Drp1and the HRES-1/Rab4-DN-induced depletion of AKAP-10 were strikingly reversed in bafilomycin-treated Jurkat cells (figure 1A), suggesting a role for increased lysosomal degradation. Along these lines, the knockdown of HRES-1/Rab4 markedly upregulated Drp1 protein levels in HeLa cells which were amenable to transfection by siRNA without loss of viability (figure 1B). As expected, the deletion of Drp1 increased mitochondrial mass in MEFs (figure 1C) which was consistent with a role for Drp1 in promoting mitophagy.[19] In the absence

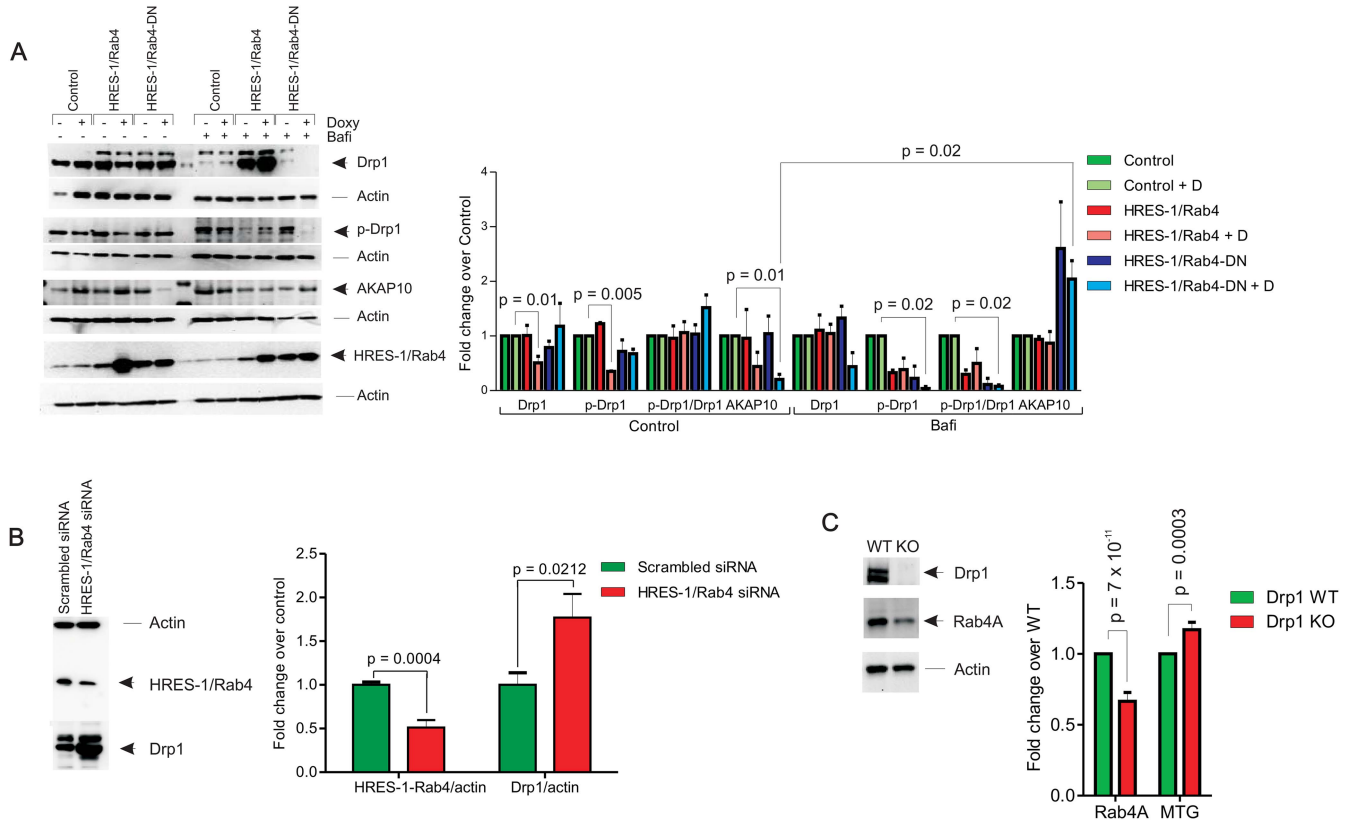

Figure 1 Depletion of Drp1 by HRES-1/Rab4. (A) Effect of HRES-1/Rab4 on Drp1 protein levels, phosphorylation of Drp1 at Ser 637, and levels of AKAP10, which regulates phosphorylation of Drp1, were evaluated in Jurkat human T cells carrying doxycyclin-inducible vectors that express wild-type HRES-1/Rab4 or dominant-negative HRES-1/Rab4^{S27N} (HRES-1/Rab4-DN). Bafilomycin reversed the depletion of Drp1 by HRES-1/Rab4 and depletion of AKAP10 by HRES-1/Rab4-DN. Left panel, representative western blots; right panel, mean±SEM of 4–6 experiments. (B) Upregulation of Drp1 protein levels by siRNA-mediated knock-down of HRES-1/Rab4. Left panel, HRES-1/Rab4 and Drp1 were analysed relative to β-actin in HeLa cells 48 h after transfection with siRNA specific for HRES-1/Rab4 nucleotides 377–399 or scrambled siRNA. Right panel, mean±SEM of five independent experiments. (C) Effect of Drp1 deletion in MEFs on Rab4 protein levels assessed by western blot and on mitochondrial mass measured by MTG fluorescence. Representative western blot (left panel) and bar chart reflect mean±SEM of 4 experiments (right panel).

of Drp1, the expression of Rab4A, the mouse homologue of HRES-1/Rab4, was diminished (figure 1C).

HRES-1/Rab4 induced the accumulation of mitochondria by inhibiting mitophagy

Next, we investigated if the HRES-1/Rab4-mediated depletion of Drp1 elicited changes in mitochondrial mass. Jurkat cells overexpressing HRES-1/Rab4 exhibited twofold greater mitochondrial mass by MTDR staining ($p=1.6\times10^{-5}$; see online supplementary figure S1A and B). Accumulation of mitochondria was also indicated by 1.7-fold elevated voltage-dependent anion channel (VDAC) protein levels in Jurkat cells overexpressing HRES-1/Rab4 ($p=0.03$; data not shown). To investigate the role of autophagy in the effect of HRES-1/Rab4 on mitochondria, we examined their association with lysosomes. The colocalisation of mitochondria with lysosomes was diminished in cells overexpressing HRES-1/Rab4 (see online supplementary figure S1). Mitochondrial mass was also increased in PBL overexpressing HRES-1/Rab4 (1.4-fold; $p=0.019$; figure 2A). Consistent with its impact on mitochondrial homeostasis, HRES-1/Rab4 was enriched in mitochondria relative to the cytosol both in Jurkat cells (not shown) and PBL (figure 2B). The partitioning of HRES-1/Rab4 to mitochondria was markedly reduced in lupus T cells relative to matched healthy controls ($-52\pm12\%$, $p=0.005$; figure 2B). The diminished localisation of mitochondria to lysosomes upon HRES-1/Rab4 overexpression in Jurkat cells, the diminished association of HRES-1/Rab4 with mitochondria in lupus PBL, and the accumulation of mitochondrial mass in Jurkat cells and PBL overexpressing HRES-1/Rab4 together suggested an underlying mechanism of inhibited mitophagy.

Stimulation of microautophagy by HRES-1/Rab4

Since early endosomes are involved in the formation of autophagosomes,[16] we examined the effect of HRES-1/Rab4 on lipidation of the microtubule-associated light chain 3 (LC3) with phosphoethanolamine, an early event of autophagosome formation.[25] While the lipidated LC3 (LC3-II) is associated with the membrane of autophagosomes, the unlipidated form of LC3 (LC3-I) resides in the cytosol[16] These studies were performed

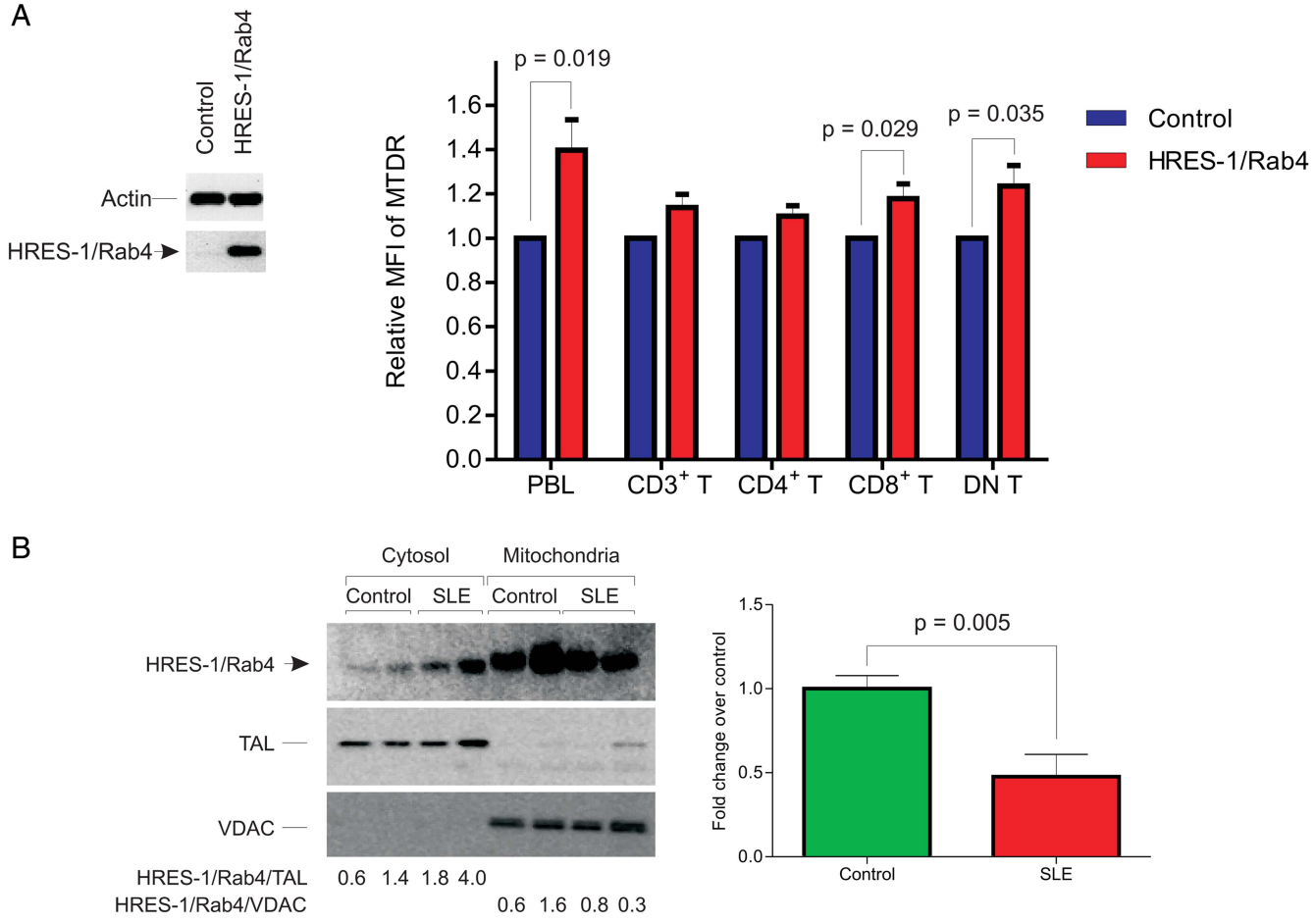

Figure 2 HRES-1/Rab4A promotes the accumulation of mitochondria in human PBL. (A) Effect of HRES-1/Rab4 overexpression on mitochondrial mass assessed in healthy control PBL stimulated with 5 μg/mL ConA for 24 h. Left panel, expression levels of adeno-associated virus (AAV)-transduced HRES-1/Rab4 was monitored by western blot. Control reflects PBL infected with AAV lacking HRES-1/Rab4 cDNA. Right panel, Assessment of mitochondrial mass by MitoTracker Deep Red (MTDR) fluorescence using flow cytometry. Data represent mean±SEM in five healthy donors. p Values reflect comparison of MTDR fluorescence in PBL infected with HRES-1/Rab4-producing AAV relative to PBL infected with control AAV using paired two-tailed t test. (B) Partitioning of HRES-1/Rab4 between the cytosol and mitochondria. Left panel, western blot analysis of HRES-1/Rab4, TAL, and VDAC in cytosolic and mitochondrial fractions of negatively isolated T cells from SLE and matched healthy subjects. Right panel, cumulative data represent mean±SE of HRES-1/Rab4 partitioning between the cytosol and mitochondria in nine lupus patients relative to the mean mitochondria/cytosol ratio of nine healthy controls normalised to 1.0.

(1) in the absence or presence of bafilomycin A1 to allow accumulation of autophagosomal proteins through blocking their maturation into autophagolysosomes and (2) in the absence or presence of rapamycin to induce autophagy.[25] Endogenous LC3-II was only detectable after treatment with bafilomycin A1 and enhanced by rapamycin (see online supplementary figure S2). LC3-II levels generated from endogenous LC3 were increased by wild-type HRES-1/Rab4 (see online supplementary figure S2A), indicating an overall stimulation of autophagy. Along this line, the generation of LC3-II from transfected FP650-LC3 fusion protein was diminished by HRES-1/Rab4-DN (see online supplementary figure S2B). The effect of HRES-1/Rab4 on the accumulation of LC3-II was not affected by rapamycin (see online supplementary figure S2A), indicating that the stimulation of autophagy by genetically enforced overexpression of HRES-1/Rab4 was not dependent on mTOR.

Drp1 expression is reduced and resistant to rapamycin treatment in SLE

Since HRES-1/Rab4 depleted the mitophagy initiator Drp1, we investigated if overexpression of HRES-1/Rab4[5] and accumulation of mitochondria in lupus T cells[26] were associated with altered expression of Drp1. As shown in figure 3, Drp1 protein levels were reduced by 86±3% in lupus PBL in comparison with matched controls (p=0.012). Diminished Drp1 levels were not corrected in SLE patients treated with rapamycin in vivo (−83±7%, p=0.017; figure 3), which was consistent with the enduring accumulation of mitochondria in rapamycin-treated patients.[7] Autophagy regulator beclin-1[18] expression was also reduced in freshly isolated SLE PBL (−56±9%, p=0.002) but reversed by rapamycin treatment (p=0.01, figure 3). Since autophagy is required for T-cell activation,[27] we investigated the capacity of lupus T cells to upregulate the expression of LC3 in response to CD3/CD28 costimulation. Indeed, the accumulation of LC3-II was 1.9-fold increased in lupus patients in comparison with healthy controls ($p=8.8\times10^{-5}$, figure 3). As expected, the LC3-II/LC3-I ratio was further enhanced by rapamycin (figure 3). In accordance with earlier findings,[7] rapamycin treatment reduced mTOR activity but did not reverse the accumulation of mitochondria in lupus T cells (data not shown). These findings suggested that the depletion of Drp1 (figure 3) along with the accumulation of mitochondria is independent of mTOR activation in SLE.

Increased expression of Rab4A and depletion of Drp1 precede accumulation of mitochondria and disease development in lupus-prone mice

To assess the involvement of Rab4A in lupus pathogenesis, we examined its expression in lupus-prone mice relative to disease development.[28 29] Disease-free mice were studied at 4 weeks of age, when we confirmed the absence of ANA, proteinuria, or nephritis. Rab4A expression was markedly increased (4.7-fold; p=0.0002; figure 4A) while Drp1 was diminished in T cells of 4-week-old female MRL/lpr mice (−54%, p=0.02; figure 4B). Expression of Rab4A was further increased at 8 weeks of age (36-fold; p=0.0005; figure 4C) when accumulation of mitochondria was evidenced by western blot detection of VDAC and MTG fluorescence in MRL/lpr mice (figure 4D). Rab4A and Drp1 protein levels were similar in naïve $CD44^{low}CD62L^{high}CD4$ T cells of B6/Lpr, MRL, and MRL/lpr mice relative to B6 controls (data not shown). Expression of Rab5, evaluated as a control Rab GTPase that mediates endocytic internalisation, was not altered in MRL/lpr, MRL, or B6/lpr relative to B6 mice (figure 4C).

At 4 weeks of age, we also observed a robust overexpression of Rab4A and depletion of Drp1 in splenocytes of female NZB/W F1 mice (figure 4E). In support of a mechanistic relationship between reciprocal changes in Rab4A and Drp1, overexpression of HRES-1/Rab4 reduced Drp1 protein levels in B6 splenocytes by −41±7.8% (p=0.034; figure 4F).

Rab4A expression was also increased in thymocytes of 4-week-old NZB/W F1 mice (see online supplementary figure S3A), showing no evidence of ANA production, proteinuria, or nephritis (data not shown). NZB/W F1 mice were also studied at 4 months and 6 months of age, when autoimmunity was detected by the production of ANA, and at 11 months of age when all mice developed nephritis of varying severity. At 4 months of age, Rab4A expression was further increased in splenocytes of NZB/W F1 mice, over 15-fold relative to age-matched B6 controls. To a lesser extent, Rab4A was overexpressed in splenocytes of 4-month-old B6.NZMSle1.Sle2.Sle3 mice (see online supplementary figure S3A). Rab5A was unchanged in splenocytes at 4 weeks of age, but it was overexpressed at 4 months of age in NZB/W F1 mice (p=0.02; see online supplementary figure S3B).

Since HRES-1/Rab4 targets CD3ζ and CD4 for lysosomal degradation, we examined this process in NZB/W F1 mice. CD3ζ expression was reduced, while CD4 expression was unchanged in T cells of 4-week-old NZB/W F1 mice in

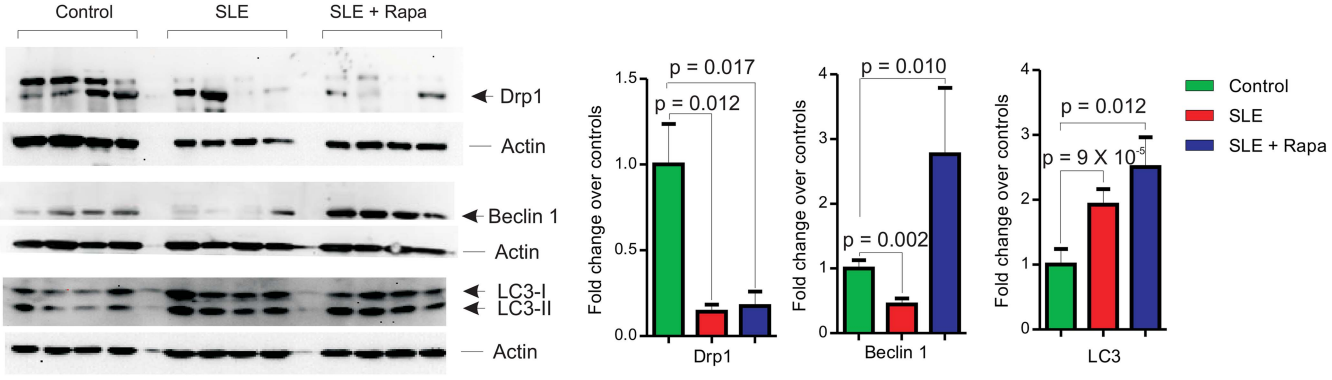

Figure 3 Assessment of Drp1, Beclin 1, and LC3 expression relative to β-actin by western blot analysis of protein lysates from PBL of healthy donors (n=12) and lupus patients treated without (n=14) or with rapamycin (n=10). Representative western blots are shown in left panels and cumulative analyses are shown in right panels. p Values <0.05 are indicated.

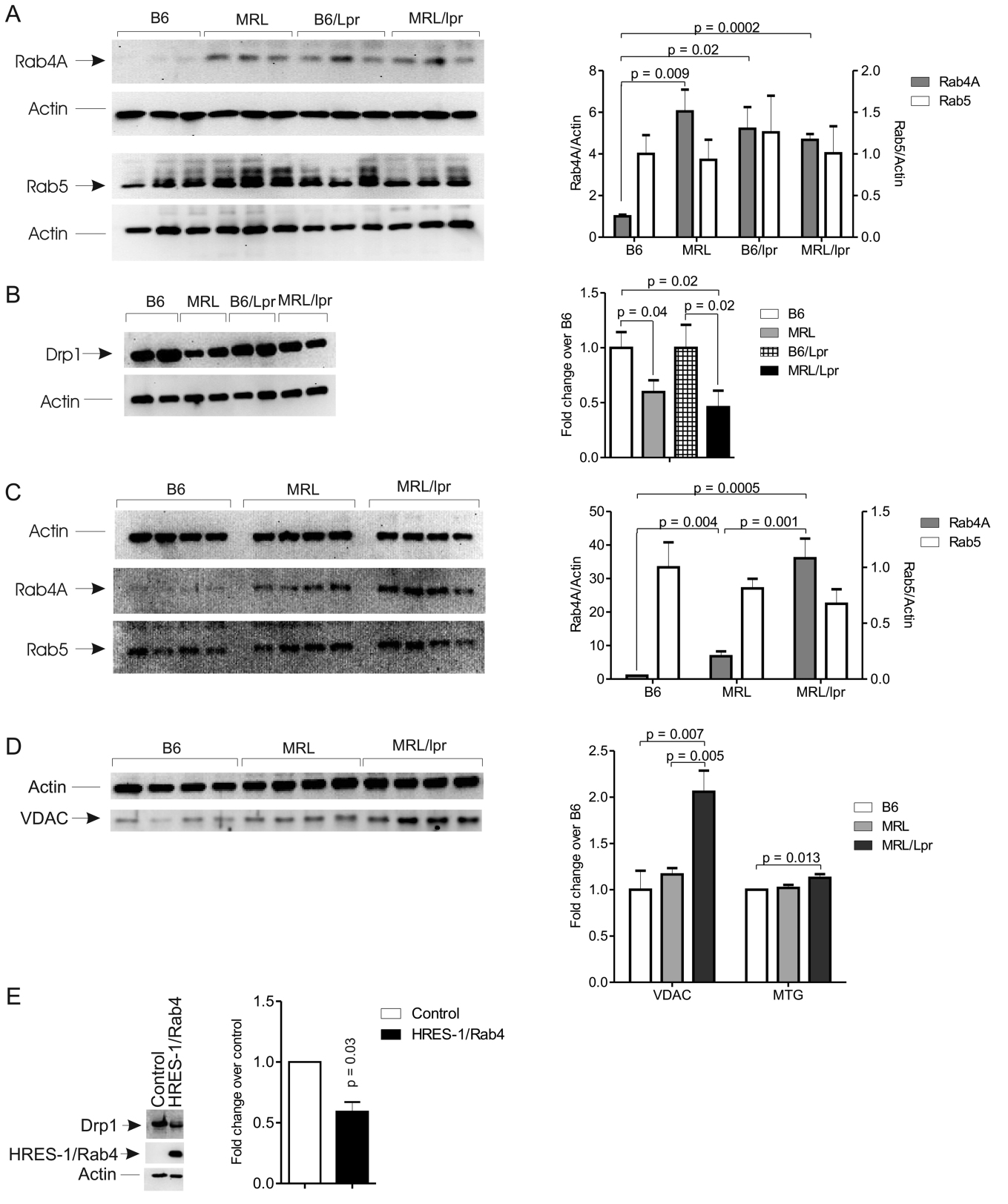

Figure 4 Increased expression of Rab4A and depletion of Drp1 in MRL/lpr and NZB/W F1 mice. (A) Western blot analysis of Rab4A and Rab5 expression in thymocytes from 4-week-old C57BL/6 (B6), MRL, C57BL/6/Lpr (B6/Lpr), and MRL/lpr mice. Representative blots are shown in the left panel, while cumulative analyses are shown in the right panel. p Values <0.05 are indicated. (B) Western blot analysis of Drp1 in negatively isolated T cells of 4-week-old mice. (C) Western blot analysis of Rab4A and Rab5 expression in splenocytes from 8-week-old mice. (D) Western blot detection of VDAC and flow cytometry of mitochondrial mass using MTG fluorescence in splenocytes of 8 week-old mice. For each parameter 4 or more mice were analysed; p values <0.05 are indicated. (E) Western blot analysis of Drp1 protein levels in B6 mouse splenocytes transduced with adeno-associated virus (AAV) expressing HRES-1/Rab4 (left panel). Data represent mean±SEM of five experiments; p values reflect comparison to cells infected with control AAV using paired two-tailed t test (right panel).

comparison with B6 controls (see online supplementary figure S3C). At 4 months of age, CD3ζ was further depleted and CD4 expression also became diminished (see online supplementary figure S3C). Beclin-1 expression was reduced in T cells from NZB/W F1 and NZW mice (see online supplementary figure S3D). Drp1 protein levels were also diminished in thymocytes of NZB/W F1 mice relative to B6 controls (see online supplementary figure S3D). Increased nitric oxide (NO) production was detectable in 4-week-old NZB/W F1 mice (see online supplementary figure S3E).

mTOR activity was not consistently elevated at 4 weeks of age but it was robustly increased in 4-month-old NZB/W F1 mice (see online supplementary figure S4). Disease progression was associated with the escalation of Rab4A overexpression, (4.3-fold at 4 weeks of age and 15.3-fold at 4 months of age) and activation of mTOR (0.8-fold at 4 weeks of age and 3.3-fold at 4 months of age; $p=0.028$ using 2-way analysis of variance) in the spleen of NZB/W F1 female mice with respect to age-matched B6 female controls (see online supplementary figure S4). A progressive decrease of mitochondrial mass was observed in B6 mice with aging (see online supplementary figure S5A). By contrast, NO production, MHP and accumulation of mitochondria, as detected by increased MTG fluorescence (see online supplementary figure S5B) and VDAC expression (see online supplementary figure S5C), were peaking in 11-month-old NZB/W F1 mice. Thus, lupus-prone mice exhibit overexpression of Rab4A, depletion of Drp1, accumulation of mitochondria, and mTOR activation, similar to patients with SLE.[5 26]

Rab geranylgeranyl transferase blockade reverses Drp1 depletion, mitochondrial accumulation, ANA production, and nephritis in lupus-prone mice

Increased Rab4A and depleted Drp1 were thus observed in 4-week-old disease-free MRL MRL/lpr and NZB/W F1 mice, indicating that these changes may represent early events in lupus pathogenesis. The accumulation of mitochondria was noted in 8-week-old MRL/lpr and 11-month-old NZB/W F1 mice. This was consistent with earlier development of autoimmunity in MRL/lpr mice.[28] To evaluate Rab4 and the pathway of endocytic recycling as target for treatment of SLE, we used a Rab geranylgeranyl transferase inhibitor 2-[3-pyridinyl]-1-hydroxyethylidene-1,1-phosphonocarboxylic acid (3-PEHPC)[30] that promoted the partitioning of HRES-1/Rab4 and Rab5 from the membrane to the cytosol compartment (see online supplementary figure S6). MRL/lpr mice were treated from 4 to 14 weeks of age, three times weekly, with subcutaneous injection of 125 μg/kg 3-PEHPC, previously found to be effective in diminishing bone resorption.[30] We compared the efficacy of 3-PEHPC to rapamycin, a potent inhibitor of lupus disease activity in mice[6] and humans.[7] Relative to the toxicity of rapamycin noted in previous studies,[31] 3-PEHPC did not elicit weight loss (figure 5A). Rapamycin-treated mice had 137 mg/dl glucose in their urine at 14 weeks of age, while 3-PEHPC-treated mice had no glucosuria ($p=0.04$). 3-PEHPC reduced ANA production, proteinuria and nephritis (figure 5A–C). Rapamycin, but not 3-PEHPC, reduced spleen mass and the expansion of $CD4^{-}CD8^{-}$ double-negative (DN) T cells (figure 6A). 3-PEHPC reduced IL-10, while rapamycin diminished IFN-γ and IL17A levels in the serum of MRL/lpr mice (figure 6B). As expected, rapamycin treatment inhibited mTOR activity (figure 6C) and reduced the numbers of $FoxP3^{+}$ cells within the CD4CD25 T-cell compartment (figure 6D) in accordance with recent findings that mTOR is required for development of Tregs in mice[32]; thus, these cells may not be responsible for suppression of autoimmunity in this model. Unlike rapamycin, 3-PEHPC did not reduce spleen mass (figure 6A),[33] expansion of DN T cells (figure 6A)[34] or mTOR activity (figure 6C). 3-PEHPC, but not rapamycin, reversed the depletion of Drp1 (figure 6E) and diminished the mitochondrial mass of B and T cells and macrophages in MRL/lpr mice (figure 6F).

DISCUSSION

The present data identify HRES-1/Rab4 as a selective regulator of autophagy, promoter of microautophagy and inhibitor of mitophagy, thus contributing to the accumulation of mitochondria and serving as a potential target for treatment in SLE (see online supplementary figure S7). The increased turnover of LC-3 and depletion of autophagy regulator Beclin 1[18] demonstrate an overall activation of microautophagy in SLE. HRES-1/Rab4 stimulates microautophagy and lysosomal degradation of proteins which are recycled through early endosomes, such as the membrane receptors CD71, CD4,[13] and CD3ζ[5] and mitophagy initiator Drp1.[17 19] We previously showed that HRES-1/Rab4 accelerated the recycling and lysosomal degradation of CD4[13] and CD3ζ but not CD8.[5] The present study uncovers that the scope of proteins targeted for lysosomal degradation by HRES-1/Rab4 includes Drp1. The depletion of Drp1 by HRES-1/Rab4 has been solely attributed to lysosomal degradation, as microarray analyses revealed no changes in Drp1 transcription in cells overexpressing HRES-1/Rab4 or HRES-1/Rab4-DN. As Drp1 is phosphorylated at Ser 637 by PKA,[19] which is anchored to endosomes via AKAP10[24] the down-regulation of AKAP-10 by HRES-1/Rab4-DN indicates that phosphorylation of Drp1 may be regulated by an interaction of HRES-1/Rab4 with AKAP10. Further studies are needed to precisely delineate the mechanism of interactions between HRES-1/Rab4, Drp1 and AKAP10.

In accordance with the role of Drp1 in initiating the fission, fragmentation and lysosomal degradation of mitochondria through mitophagy,[17 19] the depletion of Drp1 by HRES-1/Rab4 leads to increased mitochondrial mass in Jurkat cells and primary human peripheral blood T cells. The paucity of Drp1 prevents mitochondrial fission and promotes unopposed mitochondrial fusion[35] which is consistent with the formation of megamitochondria in lupus T cells.[26] The importance of mitochondrial homeostasis in lupus pathogenesis has also been supported by the recent identification of an NZB/W F1-derived lupus susceptibility gene as oestrogen-related receptor gamma, which accounts for increased mitochondrial mass that is detectable by elevated VDAC protein levels in the spleen of *Sle1c2* mice.[36]

Importantly, Rab4A, but not Rab5, was robustly overexpressed in the spleen and thymus of lupus-prone mice. The activation of Rab4A and depletion of Drp1 were detected at age of 4 weeks, well before the onset of ANA production and nephritis in NZB/W F1 or MRL/lpr mice. The overexpression of HRES-1/Rab4 led to the depletion of Drp1 both in human and murine lymphocytes, supporting a causal relationship between reciprocal changes in Rab4A and Drp1 both in lymphocytes of SLE patients and lupus-prone mice. The inactivation of Drp1 reduced Rab4A expression and increased mitochondrial mass in MEFs, which was compatible with the molecular order that overexpression of HRES-1/Rab4 and increased endocytic recycling were upstream of Drp1 depletion and mitochondrial accumulation in SLE.

Rab5 overexpression and CD4 depletion were detectable in the spleen of NZB/W F1 mice at 4 months of age, suggesting a step-wise activation of endosome recycling with progression of

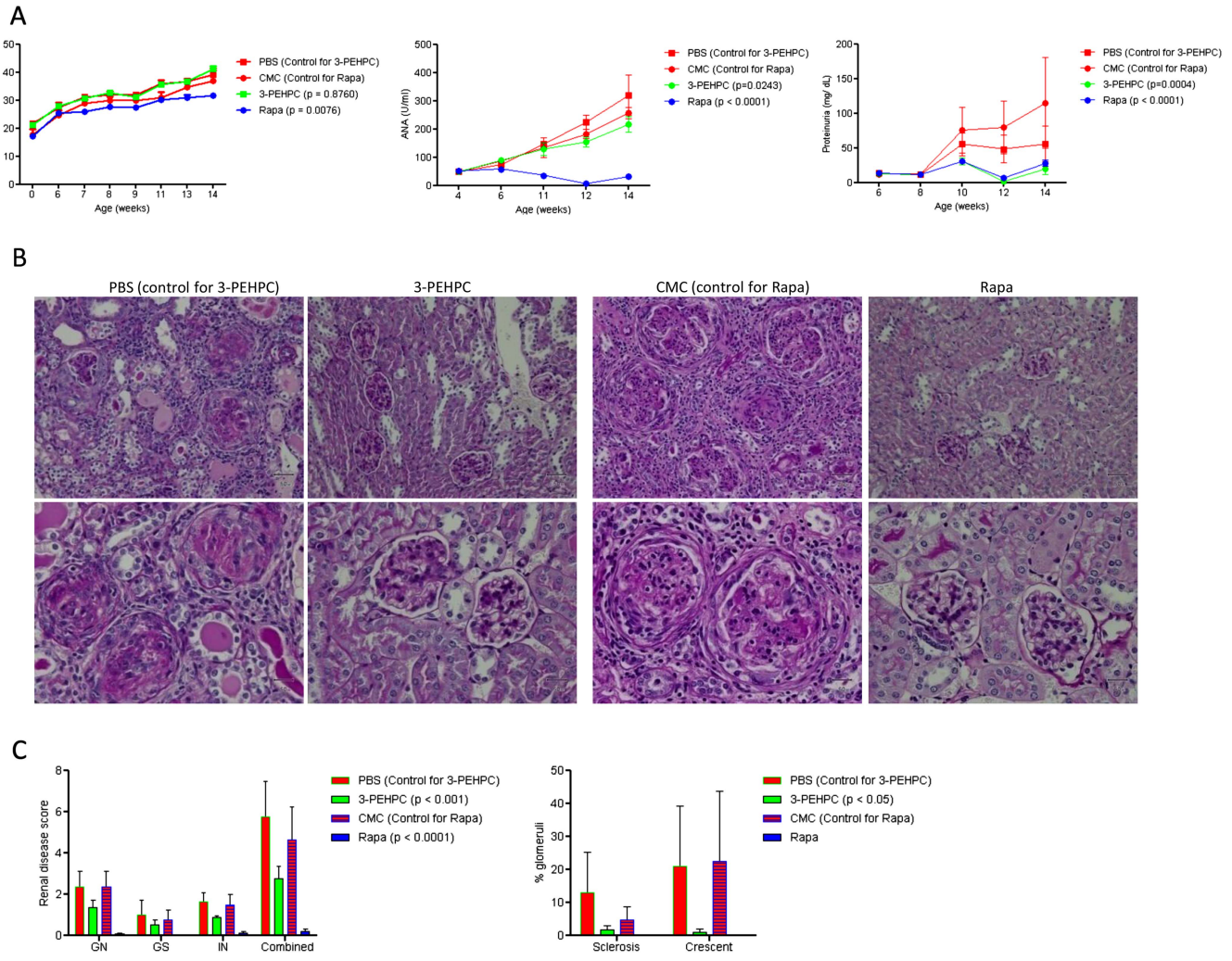

Figure 5 Effect of 3-PEHPC and rapamycin (Rapa) relative to solvent controls PBS and CMC, respectively, on autoimmunity and nephritis in MRL/lpr mice treated three times weekly, between ages of 4–14 weeks. (A) Body weight, ANA production, and proteinuria. (B) Renal pathology of 14-week-old mice. Upper and lower panels represent 200-fold and 400-fold original magnifications of identical sections; size bars represent 50 microns. PBS: GN is characterised by circumferential, predominantly cellular crescents with segmental sclerosis and hyalinosis. There are prominent interstitial lymphocytic infiltrates, tubular atrophy and protenaceous casts. 3-PEHPC: glomeruli are free of crescents. There is minimal tubular atrophy and interstitial fibrosis. CMC: glomeruli show cellular or fibrocellular crescents. Glomerular tufts are hypercellular with lobular accentuation. There is tubular atrophy and interstitial lymphocytic infiltrates and fibrosis. Rapa: normocellular glomeruli; minimal tubular atrophy and interstitial fibrosis. (C) Renal disease scores in 14-week-old MRL/lpr mice. Left panel, for each kidney, the severity of GN, GS, and IN was graded in a 0–4 semiquantitative scale. Right panel, numbers of glomeruli with sclerosis and/or crescent formation were determined and expressed as a percentage of total glomeruli observed in the entire cortical field. p values <0.05 reflect two-way analysis of variance.

disease pathogenesis and mimicking the reciprocal overexpression of small GTPases HRES-1/Rab4 and Rab5 and depletion of CD4 and CD3ζ in T cells of SLE patients.[5] We found that expression levels of Rab4A and Drp1 in naïve CD4 T cells of B6 mice were not different relative to those of B6/Lpr, MRL and MRL/lpr mice (data not shown). CD3/CD28 costimulation for 24 h reduced Drp1 levels in human PBL by 80.8±9.4% (p=0.007; data not shown). As earlier documented, CD3/CD28 costimulation increased HRES-1/Rab4 protein levels in human T cells.[5] These findings indicate that Rab4A overexpression and Drp1depletion may depend on T-cell activation in SLE. Increased production of NO during T-cell activation[37] which induces the expression of HRES-1/Rab4 in vitro,[5] may underlie the overexpression of Rab4A in 4-week-old NZB/W F1 mice. Lupus-associated polymorphic haplotypes within the long terminal repeat-enhancer[12] also influence expression of HRES-1/Rab4 in human T cells.[13]

Blocking of Rab geranylgeranyl transferase activity with 3-PEHPC prevented Drp1 depletion, accumulation of mitochondria in T and B cells, ANA production and nephritis, indicating that activation of the endocytic recycling machinery contributes to the pathogenesis of SLE. The reversal Drp1 depletion by 3-PEHPC may influence T-cell activation through positioning of mitochondria at the immunological synapse[38] Mitochondria serve as a buffer for the management of T-cell activation-induced Ca^{2+} fluxing,[26] and Drp1-dependent fragmentation of the mitochondrial network may protect T cells from hyperactive Ca^{2+} signalling.[38] This mechanism is supported by the reduction of cytosolic Ca^{2+} in T cells of 3-PEHPC-treated MRL/lpr mice (data not shown). Interestingly, rapamycin failed to reverse Drp1 depletion or to reduce mitochondrial mass, suggesting that the accumulation of mitochondria is mTOR-independent. These findings are consistent with the persistence of MHP and accumulation of mitochondria in T

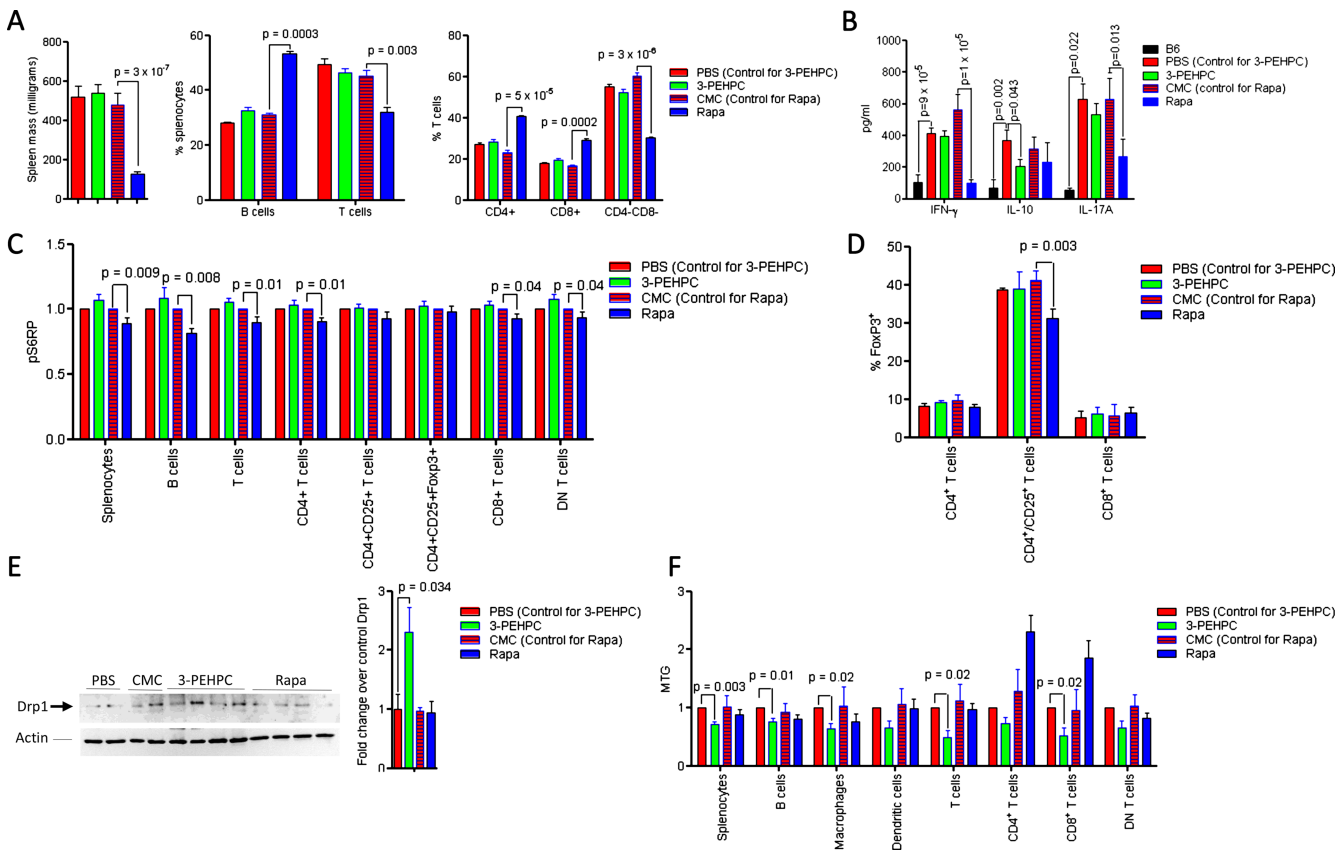

Figure 6 Effect of 3-PEHPC and Rapa relative to solvent controls PBS and CMC, respectively, on the immune system and mitochondrial homeostasis of MRL/lpr mice treated weekly between ages of 4–14 weeks, as described under figure 5. (A) Effect of 3-PEHPC and Rapa on spleen size, B and T cells, as well as CD4, CD8 and DN T-cell frequencies. (B) Effect of 3-PEHPC and Rapa treatment on IFN-γ, IL-10, and IL-17A levels in serum of 14-week-old MRL/lpr mice. (C) Effect of 3-PEHPC and Rapa treatment on mTOR activity in spleen subsets of 14-week-old MRL/lpr mice. (D) Effect of 3-PEHPC and Rapa treatment on Foxp3 expression in CD4, CD4/CD25 and CD8 T cells. (E) Prevention of Drp1 depletion by 3-PEHPC in 14-week-old MRL/lpr mice. Representative (left panel) and cumulative western blot analyses of negatively isolated T cells from MRL/lpr mice-treated PBS, CMC, 3-PEHPC and Rapa (right panel). (F) Effect of 3-PEHPC and Rapa treatment on mitochondrial mass (MTG) in spleen lymphocyte subsets of 14-week-old MRL/lpr mice. p Values <0.05 reflect comparison with unpaired two-tailed t test.

cells of SLE patients upon mTOR blockade with rapamycin[5 7] or NAC.[8]

In addition to the distinct impact on mitochondrial homeostasis, the cytokine profile of MRL/lpr mice was also differentially influenced by 3-PEHPC and rapamycin. The production of IFN-γ and IL17A, but not of IL-10, was reduced by rapamycin in accordance with a dominant role of mTOR in Th1 and Th17 T-cell development.[39] By contrast, 3-PEHPC failed to influence IFN-γ and IL17A, but reduced levels of IL-10 that have been widely implicated in pathogenesis of human lupus.[40–42] The diminished production of IL-10 may be related to the impact of 3-PEHPC on non-T cells, such as B cells and macrophages. Although 3-PEHPC inhibited the membrane partitioning of HRES-1/Rab4 and Rab5, it may likely influence other Rab GTPases. Therefore, further investigations into the role of HRES-1/Rab4 in lupus pathogenesis appear warranted in genetically altered animals.

In summary, our findings provide evidence for a role of HRES-1/Rab4-mediated Drp1 depletion in altered mitochondrial homeostasis in both SLE patients and lupus-prone mice. Rab geranylgeranyl transferase blockade with 3-PEHPC reversed the depletion of Drp1, accumulation of mitochondria, ANA production and nephritis in lupus-prone mice, identifying the regulation of mitochondrial homeostasis by HRES-1/Rab4 as a mechanism of pathogenesis and potential target for treatment in SLE.

Author affiliations
[1]Departments of Medicine, Microbiology, and Immunology, Biochemistry and Molecular Biology, Neuroscience and Physiology, and Pathology, SUNY Upstate Medical University, Syracuse, New York, USA
[2]Department of Pathology, Cedars-Sinai Medical Center, Los Angeles, California, USA
[3]Department of Medicine, Medical College of Georgia, Augusta, Georgia, USA
[4]Department of Medicine, UCLA, Los Angeles, California, USA
[5]Shemiakin-Ovchinnikov Institute of Bioorganic Chemistry, RAS, Moscow, Russia
[6]Department of Experimental Medicine, University of Rome, Rome, Italy

Acknowledgements This work was supported in part by grants AI048079 and AI072648 from the National Institutes of Health, the Alliance for Lupus Research, and the Central New York Community Foundation. The authors thank Dr Frank Ebetino for providing 3-PEHPC, Drs Katsuyoshi Mihara and David Chan for providing Drp1-deficient mouse embryonic fibroblasts, and Dr Paul Phillips for encouragement and support.

Contributors All authors meet contributorship requirements.

Funding National Institutes of Health, the Alliance for Lupus Research, and the Central New York Community Foundation.

Competing interests None.

Ethics approval SUNY IRB.

Provenance and peer review Not commissioned; externally peer reviewed.

REFERENCES

1 Gergely PJ, Grossman C, Niland B, *et al*. Mitochondrial hyperpolarization and ATP depletion in patients with systemic lupus erythematosus. *Arth Rheum* 2002;46:175–90.
2 Perl A, Gergely P Jr., Nagy G, *et al*. Mitochondrial hyperpolarization: a checkpoint of T cell life, death, and autoimmunity. *Trends Immunol* 2004;25:360–7.
3 Perl A. Systems biology of lupus: Mapping the impact of genomic and environmental factors on gene expression signatures, cellular signaling, metabolic pathways, hormonal and cytokine imbalance, and selecting targets for treatment. *Autoimmunity* 2010;43:32–47.
4 Desai BN, Myers BR, Schreiber SL. FKBP12-rapamycin-associated protein associates with mitochondria and senses osmotic stress via mitochondrial dysfunction. *Proc Natl Acad Sci USA* 2002;99:4319–24.
5 Fernandez DR, Telarico T, Bonilla E, *et al*. Activation of mTOR controls the loss of TCR. in lupus T cells through HRES-1/Rab4-regulated lysosomal degradation. *J Immunol* 2009;182:2063–73.
6 Warner LM, Adams LM, Sehgal SN. Rapamycin prolongs survival and arrests pathophysiologic changes in murine systemic lupus erythematosus. *Arth Rheum* 1994;37:289–97.
7 Fernandez D, Bonilla E, Mirza N, *et al*. Rapamycin reduces disease activity and normalizes T-cell activation-induced calcium fluxing in patients with systemic lupus erythematosus. *Arth Rheum* 2006;54:2983–8.
8 Lai Z-W, Hanczko R, Bonilla E, *et al*. N-acetylcysteine reduces disease activity by blocking mTOR in T cells of lupus patients. *Arth Rheum* 2012;64:2937–46.
9 Enyedy EJ, Nambiar MP, Liossis SN, *et al*. Fc epsilon receptor type I gamma chain replaces the deficient T cell receptor zeta chain in T cells of patients with systemic lupus erythematosus. *Arth Rheum* 2001;44:1114–21.
10 Sancak Y, Peterson TR, Shaul YD, *et al*. The Rag GTPases Bind Raptor and Mediate Amino Acid Signaling to mTORC1. *Science* 2008;320:1496–501.
11 Magistrelli C, Samoilova E, Agarwal RK, *et al*. Polymorphic genotypes of the HRES-1 human endogenous retrovirus locus correlate with systemic lupus erythematosus and autoreactivity. *Immunogenetics* 1999;49:829–34.
12 Pullmann RJr, Bonilla E, Phillips PE, *et al*. Haplotypes of the HRES-1 endogenous retrovirus are associated with development and disease manifestations of systemic lupus erythematosus. *Arth Rheum* 2008;58:532–40.
13 Nagy G, Ward J, Mosser DD, *et al*. Regulation of CD4 Expression via Recycling by HRES-1/RAB4 Controls Susceptibility to HIV Infection. *J Biol Chem* 2006;281:34574–91.
14 Tsao BP. Lupus susceptibility genes on human chromosome 1. *Int Rev Immunol* 2000;19:319–34.
15 Sengupta S, Peterson TR, Sabatini DM. Regulation of the mTOR Complex 1 Pathway by Nutrients, Growth Factors, and Stress. *Mol Cell* 2010;40:310–22.
16 Tooze SA, Jefferies HBJ, Kalie E, *et al*. Trafficking and signaling in mammalian autophagy. *IUBMB Life* 2010;62:503–8.
17 Weidberg H, Shvets E, Elazar Z. Biogenesis and Cargo Selectivity of Autophagosomes. *Ann Rev Biochem* 2011;80:125–56.
18 Chen Y, Klionsky DJ. The regulation of autophagy—unanswered questions. *J Cell Sci* 2011;124:161–70.
19 Gomes LC, Benedetto GD, Scorrano L. During autophagy mitochondria elongate, are spared from degradation and sustain cell viability. *Nat Cell Biol* 2011;13:589–98.
20 Tan EM, Cohen AS, Fries JF, *et al*. The 1982 revised criteria for the classification of systemic lupus erythematosus. *Arth Rheum* 1982;25:1271–7.
21 Hochberg MC. Updating the American College of Rheumatology revised criteria for the classification of systemic lupus erythematosus. *Arth Rheum* 1997;40:1725.
22 Perl A, Gonzalez-Cabello R, Lang I, *et al*. Effector activity of OKT4+ and OKT8+ T-cell subsets in lectin- dependent cell-mediated cytotoxicity against adherent HEp-2 cells. *Cell Immunol* 1984;84:185–93.
23 Ishihara N, Nomura M, Jofuku A, *et al*. Mitochondrial fission factor Drp1 is essential for embryonic development and synapse formation in mice. *Nat Cell Biol* 2009;11:958–66.
24 Eggers CT, Schafer JC, Goldenring JR, *et al*. D-AKAP2 interacts with Rab4 and Rab11 through its RGS domains and regulates transferrin receptor recycling. *J Biol Chem* 2009;284:32869–80.
25 Mizushima N, Yoshimori T, Levine B. Methods in Mammalian Autophagy Research. *Cell* 2010;140:313–26.
26 Nagy G, Barcza M, Gonchoroff N, *et al*. Nitric Oxide-Dependent Mitochondrial Biogenesis Generates Ca2+ Signaling Profile of Lupus T Cells. *J Immunol* 2004;173:3676–83.
27 Hubbard VM, Valdor R, Patel B, *et al*. Macroautophagy regulates energy metabolism during effector T cell activation. *J Immunol* 2010;185:7349–57.
28 Peng SL. Experimental use of murine lupus models. In: Perl A. ed. *Methods in molecular medicine: autoimmunity methods and protocols*. Totowa: Humana, 2005:227–72.
29 Kono DH, Theofilopoulos AN. Genetics of systemic autoimmunity in mouse models of lupus. [Review] [84 refs]. *Int Rev Immunol* 2000;19:367–87.
30 Lawson MA, Coulton L, Ebetino FH, *et al*. Geranylgeranyl transferase type II inhibition prevents myeloma bone disease. *Biochem Biophys Res Commun* 2008;377:453–7.
31 Yang SB, Lee H, Young D, *et al*. Rapamycin induces glucose intolerance in mice by reducing islet mass, insulin content, and insulin sensitivity. *J Mol Med* 2012;90:575–85.
32 Wang Y, Camirand G, Lin Y, *et al*. Regulatory T cells require mammalian target of rapamycin signaling to maintain both homeostasis and alloantigen-driven proliferation in lymphocyte-replete mice. *J Immunol* 2011;186:2809–18.
33 Huynh H, Chow PK, Palanisamy N, *et al*. Bevacizumab and rapamycin induce growth suppression in mouse models of hepatocellular carcinoma. *J Hepatol* 2008;49:52–60.
34 Teachey DT, Obzut DA, Axsom K, *et al*. Rapamycin improves lymphoproliferative disease in murine autoimmune lymphoproliferative syndrome (ALPS). *Blood* 2006;108:1965–71.
35 Twig G, Elorza A, Molina AJA, *et al*. Fission and selective fusion govern mitochondrial segregation and elimination by autophagy. *EMBO J* 2008;27:433–46.
36 Perry DJ, Yin Y, Telarico T, *et al*. Murine Lupus Susceptibility Locus Sle1c2 Mediates CD4+ T Cell Activation and Maps to Estrogen-Related Receptor gamma. *J Immunol* 2012;189:793–803.
37 Nagy G, Koncz A, Perl A. T cell activation-induced mitochondrial hyperpolarization is mediated by Ca^{2+}- and redox-dependent production of nitric oxide . *J Immunol* 2003;171:5188–97.
38 Baixauli F, Martin-Cofreces NB, Morlino G, *et al*. The mitochondrial fission factor dynamin-related protein 1 modulates T-cell receptor signalling at the immune synapse. *EMBO J* 2011;30:1238–50.
39 Delgoffe GM, Pollizzi KN, Waickman AT, *et al*. The kinase mTOR regulates the differentiation of helper T cells through the selective activation of signaling by mTORC1 and mTORC2. *Nat Immunol* 2011;12:295–304.
40 Georgescu L, Vakkalanka RK, Elkon KB, *et al*. Interleukin-10 promotes activation-induced cell death of SLE lymphocytes mediated by Fas ligand. *J Clin Invest* 1997;100:2622–33.
41 Gergely PJ, Niland B, Gonchoroff N, *et al*. Persistent mitochondrial hyperpolarization, increased reactive oxygen intermediate production, and cytoplasmic alkalinization characterize altered IL-10 signaling in patients with systemic lupus erythematosus. *J Immunol* 2002;169:1092–101.
42 Sharif MN, Tassiulas I, Hu Y, *et al*. IFN-alpha priming results in a gain of proinflammatory function by IL-10: implications for systemic lupus erythematosus pathogenesis. *J Immunol* 2004;172:6476–81.

SUPPLEMENTAL MATERIALS

SUPPLEMENTAL METHODS

Human subjects. A total of 38 patients with systemic lupus erythematosus (SLE) were investigated. All patients satisfied the criteria for a definitive diagnosis [1;2]. Disease activity was assessed by SLEDAI score [3]. Seventeen patients were treated with rapamycin with therapeutic target of plasma concentrations at 6-15 ng/ml (mean age: 38.6 ± 15 years, ranging between 21-65 years; SLEDAI: 6.9 ± 3.7). 15 patients were Caucasian females, 1 patient was Caucasian male, and 1 patient was African-American female. Among the 21 remaining SLE patients treated without rapamycin, 10 were receiving prednisone, 10 were receiving mycophenolic acid, 8 were receiving mycophenolate mofetil, 2 were receiving 6-mercaptopurine, 1 was receiving cyclosporin A. Their mean age was 45.4 ± 14 years, ranging between 18-69 years; SLEDAI: 6.7 ± 4.4. As controls, 21 healthy subjects were studied
in parallel, matched for gender, ethnicity, and age of SLE patients for each blood donation. 17 controls were Caucasian females, 3 controls were Caucasian males, and 1 control was African-American female. The study has been approved by the Institutional Review Board for the Protection of Human Subjects.

Separation and culture of human peripheral blood lymphocytes. Peripheral blood mononuclear cells (PBMC) were isolated from heparinized venous blood on Ficoll-Hypaque gradient. Peripheral blood lymphocytes (PBL) were separated from monocytes by adherence to autologous serum-coated Petri dishes [4]. T cells (>95% CD3+) were negatively isolated from PBMC with Dynal magnetic beads conjugated to IgG antibodies for CD14, CD16 HLA class II DR/DP, CD56 and CD235a; Invitrogen Cat No.113-11D). CD4+ T cells (>98% CD4+) were negatively isolated with magnetic beads conjugated to IgG antibodies for CD8, CD14, CD16, HLA class II DR/DP, CD56, CDw123, and CD235a (Invitrogen Cat No.113-39D). The resultant cell population was resuspended at 10^6 cells/ml in RPMI 1640 medium, supplemented with 10% fetal calf serum (FCS), 2 mM L-glutamine, 100 IU/ml penicillin, and 100 µg/ml gentamicin in 12-well plates at 37^{o}C in a humidified atmosphere with 5% CO_2. Cross-linking of the CD3 antigen was performed by addition of cells to plates pre-coated with 100 µg/ml goat anti-mouse IgG (Jackson, West Grove, PA) for 2 h and, after washing, pre-coated with 1 µg/ml OKT3 monoclonal antibody (CRL 8001 from ATCC, Rockville, MD) for 1 h at 37^{o}C. CD28 co-stimulation was performed by addition of 500 ng/ml mAb CD28.2 (Pharmingen, San Diego, CA). In vitro treatments of PBL or negatively isolated T cells was performed with rapamycin (50 nM dissolved in DMSO, Cell Signaling Cat# 9904) and bafilomycin A1, used as a lysomomal inhibitor to facilitate detection of proteins (200 nM; Calbiochem).

Mouse embryonic fibroblasts (MEFs). MEFs deficient in Drp1 [5] were provided by Drs. Katsuyoshi Mihara (Kyushu University) and David Chan (California Institute of Technology) and cultured in DMEM medium supplemented with 10% FBS, 2 mM L-glutamine, 100 U/mL penicillin, 100 µg/mL streptomycin, 10 µg/mL amphotericin B, 1% MEM non-essential amino acid solution (10 mM, InVitrogen), and 1 mM sodium pyruvate [5].

Mice. Female New Zealand White (NZW), New Zealand White x New Zealand Black F1 (NZB/W F1), B6.NZMSle1/Sle2/Sle3, MRL, MRL/lpr, C57BL/6 (B6), and C57BL/6.Lpr (B6/Lpr) mice were obtained from Jackson laboratories (Bar Harbor, ME). Female NZB/W F1 mice and age-matched Balb C/NZW and B6 controls were received from Dr. Ram Singh at

University of California Los Angeles. Animal experimentation has been approved by the Committee on the Human Use of Animals in accordance with NIH Guide for the Care and Use of Laboratory Animals.

Isolation of mouse lymphocyte subsets. The harvested spleen tissue was filtered through a 70-μm cell strainer and splenocytes were recovered in DMEM medium, supplemented with 10% fetal calf serum (FCS), 2 mM L-glutamine, 100 IU/ml penicillin, and 100 μg/ml gentamicin. ACK buffer (0.15 M NH_4Cl, 10mM $KHCO_3$, 1 mM Na_2EDTA) was used for lysing of red blood cells for 5 minutes at room temperature. CD3 T cells (Cat # 114.13D), CD4 T cells (Cat# 11461D), CD8 T cells (Cat# 11462D), and B cells (Cat# 11422D) were isolated with magnetic beads following the manufacturer's instructions (InVitrogen, Carlsbad, CA). Naïve $CD44^{low}CD62L^{high}$ $CD4^+$ T cells were isolated with the EasySep protocol (StemcellTechnologies, Vancouver, BC, Canada; Cat #19765). 85-95% purity of cell separations was confirmed for each isolation by flow cytometry.

Flow cytometric analysis of mitochondrial transmembrane potential ($\Delta\Psi_m$) and mitochondrial mass, and nitric oxide. $\Delta\Psi_m$ was estimated by staining for 15 min at 37°C in the dark with 1 μM TMRM (excitation: 543 nm, emission: 567 nm recorded in FL-2) and 20 nm 3,3'-dihexyloxacarbocyanine iodide ($DiOC_6$, excitation: 488 nm, emission: 525 nm recorded in FL-1). Co-treatment with a protonophore, 5 μM carbonyl cyanide m-chlorophenylhydrazone (mClCCP, Sigma) for 15 min at 37°C resulted in decreased TMRM and $DiOC_6$ fluorescence and served as a positive control for disruption of mitochondrial transmembrane potential [6]. Mitochondrial mass was monitored by staining with 100 nM MitoTracker Green-FM (excitation: 490 nm, emission: 516 nm recorded in FL-1) or 100 nM MitoTracker Deep Red (MTDR, excitation: 644 nm, emission: 665 nm). Production of nitric oxide (NO) was assessed by using 4-amino-5-methylamino-2',7'-difluoroflourescein diacetate (DAF-FM; excitation: 495 nm, emission: 518 nm, recorded in FL-1). Measurement of NO was calibrated by incubating PBL with NO donors NOC-18 (200 μM to 1.8 mM) or sodium nitroprusside (SNP; 400 μM to 10 mM), as earlier described [7]. All above fluorescent probes were obtained from Invitrogen/Molecular Probes (Eugene, OR). Diaminorhodamine-4M was used to evaluate peroxynitrite production (DAR-4M, Calbiochem, San Diego, CA; excitation 544 nm, emission 590 nm). Samples were analyzed using a Becton Dickinson LSRII flow cytometer equipped with 20 mW solid-state Ng-YAG (emission at 355 nm), 20 mW argon (emission at 488 nm), 10 mW diode-pumped solid-state yellow-green (emission at 535 nm), and 16 mW helium-neon lasers (emission at 634 nm). Data were analyzed with Flow Jo software (TreeStar Corporation, Ashland, OR). Dead cells and debris were excluded from the analysis by electronic gating of forward (FSC) and side scatter (SSC) measurements. Each measurement was carried out on ≥ 10,000 cells. In each experiment, freshly isolated control and lupus cells were analyzed in parallel. Detailed protocols for assessment of mitochondrial dysfunction in SLE have been recently described [8].

Microarray analysis of gene expression. RNA was extracted from Jurkat cells carrying doxycycline-inducible GFP-producing control, HRES-1/Rab4 and GFP-producing expression vector (HRES-1/Rab4), or dominant- negative HRES-1/$Rab4^{S27N}$ and GFP-producing expression vector after incubation with or without doxycycline for 24 h (HRES-1/Rab4-DN). Biotinylated cRNA was produced by in vitro transcription and hybridized to Affymetrix HG-U133 Plus-2

chips with 54,675 probe sets, as earlier described [9;10]. Log2-based normalized data were evaluated for opposing doxycycline-induced changes in gene expression in cells expressing HRES-1/Rab4 versus HRES-1/Rab4^{S27N} at 99.99% confidence interval. Fold changes relative to the mean were displayed in heat diagrams [11]. Pathway analysis was performed using Strings 9.0 protein-protein interaction predictor software (http://string-db.org) and false discovery rate (FDR) p values were determined with Bonferrroni correction.

Western blot analyses. Whole cell protein lysates were prepared by lysis in radio-immunoprecipitation assay buffer (150 mM NaCl, 2% NP-40, 0.5% sodium deoxycholate, 0.1% SDS, 50 mM Tris pH 8.0, 1 mM PMSF, 1 μg/ml aproptinin, 1 μg/ml pepstatin, 1 μg/ml leupeptin, 1 mM NaF, 1 mM sodium orthovanadate, 0.1 mM sodium molybdate, 10 mM sodium pyrophosphate) at a density of 4 x 10^7 cells/ml on ice, followed by addition of equal volumes of Laemmli protein sample buffer (60 mM Tris-Cl pH 6.8, 2% SDS, 10% glycerol, 5% β-mercaptoethanol, 0.01% bromophenol blue) and heated to 95°C for 5 minutes prior to separation on SDS-PAGE gels and transfer to 0.45 μm nitrocellulose membranes. HRES-1/Rab4 was detected by primary rabbit antibodies directed to the C-terminus (Santa Cruz sc-312) and Ab 13407 directed to full-length native protein [12]. Expression of HRES-1/Rab4$^{1-121}$ was detected by G1432 rabbit antibody directed to peptide residues 100-121 (Genemed, San Antonio, TX). Rab4B was detected with mouse monoclonal IgM antibody (sc-271982) and goat polyclonal IgG antibody (Santa Cruz cat # sc-26565). We found dominant expression on the protein level of the full-length 218-amino-acid-long HRES-1/Rab4 coding gene in human lymphocytes [12] and the synthenic Rab4A gene in mouse lymphocytes, respectively; GenBank™ accession number AY585832. All expression and gene transduction data on HRES-1/Rab4 in this paper refer to this gene product.

mTOR (#2972), phospho-mTOR (Ser 2448, #2971), 4E-BP1 (#9644), phospho-4E-BP1 (Thr 37/46, #2855), pan-Akt (#4685), phospho-Akt (Ser 473, #4058), phospho-Drp1 (Ser 637, #6319), TSC1 (#4906), TSC2 (#3990), Raptor (#2280), mLST8 (#3274), LC3A/B (#4108), and LC3B (#2775) antibodies were obtained from Cell Signaling. Rab4A (sc-312), Drp1 (sc-32898), p70 S6 kinase (sc-8418), phospho-p70 S6 kinase (Thr 389, sc-8416), and Beclin-1 (sc-11427) antibodies were from Santa Cruz Biotechnology. Rictor antibody (#A500-002A) was from Bethyl laboratories. VDAC1 (ab61273) and Rab5 (ab18211) antibodies were from Abcam. AKAP10 antibody (NBP1-56509) was from Novus Biologicals. Antibodies to human and mouse TCR/CD3ζ (sc-1239) and mouse CD4 (sc-7219) were obtained from Santa Cruz. Human CD4 was detected with monoclonal mouse antibody 4B12 from Novocastra/Leica (NCL-L-CD4-368). Reactivities to primary antibodies were detected with horseradish peroxidase-conjugated secondary antibodies (Jackson, West Grove, PA) and visualized by enhanced chemiluminescence (Western Lightning Chemiluminescence Reagent Plus, GE Health Care/PerkinElmer Life Sciences, Inc., Boston, Massachusetts). Automated densitometry was used to quantify the relative levels of protein expression using a Kodak Image Station 440CF with Kodak 1D Image Analysis Software (Eastman Kodak Company, Rochester, NY).

Confocal microscopy. Lysosomal compartments were labeled by incubating cells at 37°C with 5uM LysoTracker Red (excitation: 577 nm, emission: 590 nm, Invitrogen cat #: L7528) for 30 minutes in complete RPMI. Mitochondria were visualized by staining with 100 nM MitoTracker Deep Red (MTDR, excitation: 644 nm, emission: 665 nm, Invitrogen cat#: M22426). Cells were washed twice and resuspended in 37°C RPMI and allowed to adhere to positively charged

coverslips for 10 minutes, followed by fixation in 4% paraformaldehyde-phosphate buffered saline solution. Visualization of the specimens on the slides was carried out under a Zeiss 510 LSM Meta confocal microscope using Zeiss LSM Image Browser software version 4.2 (Carl Zeiss Microimaging, Thornwood, NJ).

Autophagy induction. Autophagy was induced by treatment with 50 nM rapamycin in the presence and absence of lysosomal inhibitors (200 nM bafilomycin A1, 500 nM folimycin, or 100 μM chloroquine), or protease inhibitors (10 μg/ml leupeptin, 10 μg/ml pepstatin A, or 10 μg/ml E64d) [13]. Autophagy was evaluated in PBL from healthy controls, SLE patients treated without or with rapamycin *in vivo* after stimulation with plate-bound CD3 and soluble CD28 antibodies for 7 days with 200 nM bafilomycin A1 added for lysosomal blockade in the last 24 hours.

Transduction of HRES-1/Rab4 by adeno-associated virus (AAV). HRES-1/Rab4 cDNA was cloned upstream of the internal ribosomal entry site (IRES) sequence in pAAV-IRES-GFP vector (Stratagene, La Jolla, CA) as described previously [12]. Replication-defective virus was produced by co-transfection of AAV-293 cells with control or HRES-1/Rab4 containing pAAV-IRES-GFP vector, pAAV-RC, and pHelper plasmids, 30 μg of each plasmid. Calcium phosphate precipitation was used for transfection, in which 0.3M calcium chloride and 2X HBS solution (NaCl, Na_2HPO_4, HEPES pH 7.1) were added to 90 μg of plasmid DNAs, mixed by bubbling through a Pasteur pipette, and added drop-wise to AAV-293 cells plated in T-175 flasks at 70-80% confluency. Culture medium was replaced 6 hours post-transfection and cells were incubated at 37°C in 5% CO_2.

Virus was collected, filtered, and concentrated 72 h post-transfection. AAV-293 cells and culture medium were transferred to polypropylene tubes through scraping flasks with a rubber policeman. Four freeze-thaw cycles were used to release cell-associated virions by transferring samples from dry ice-100% ethanol to a 37°C water bath. Cellular debris was pelleted by centrifugation in a Sorvall RC-5B refrigerated superspeed centrifuge (Du Pont Instruments, Wilmington, DE) at 10,000 x g for 20 min at 4°C. Supernatants were filtered twice through 5 μm and 0.8 μm Millex SV syringe filters and layered onto 15 ml of Amicon Ultrafree CL centrifugal filter units (Millipore Cat No. UFC4BHK25, Burlington, MA). Samples were centrifuged in a Beckman Allegra 6KR centrifuge (Beckman-Coulter, Indianapolis, IN) at 5000 x g for 30 minutes at room temperature to concentrate viral supernatants. Concentrated virus preparations were frozen at -80°C until use.

Concentrated AAV supernatants were used to infect PBL from healthy controls, SLE patients, and negatively-isolated mouse T cells for 24-48 hours. GFP expression was measured by flow cytometry and equilibrated among constructs. (excitation: 488 nm, emission: 509 nm; FL1 channel). Optimal GFP expression occurred at 48 h post infection of PBL with >99% of cells infected. Mouse T cells were analyzed 24 h post infection, due to a decline in cell viability at 48 h. Over-expression of HRES-1/Rab4 by AAV transduction was confirmed by western blotting using antibody directed to the C-terminus of Rab4A (Santa Cruz, catalog #sc-312).

In vitro prenylation assay. Prenylation of HRES-1/Rab4 and Rab5 was evaluated by western blot analysis of soluble and insoluble fractions from Triton X 114-treated Jurkat cell extracts, as earlier described [14]. Triton X-114 separates hydrophilic proteins from amphiphilic proteins so that lipophilic prenylated Rabs partition to the detergent-rich phase, while unprenylated Rabs

remain in the aqueous phase. Jurkat 6678 cells transfected with wild-type HRES-1/Rab4 and induced with doxycycline for 24 hours in the absence or presence of 500 μM 3-PEHPC or 2 mM 3-PEHPC at 37°C at a cell density of 0.5 million cells/ml. Cells were washed by centrifugation at 1,000 x g in PBS and pellets were lysed in Triton X-114 buffer (20 mM Tris, 150 mM NaCl, 1% Triton X-114, pH 7.5). Lysates were cleared by centrifugation at 13,000 x g for 15 minutes. The supernatant was then incubated at 37°C for 10 minutes, followed by centrifugation at 13,000 x g for 2 minutes. The aqueous supernatant was used as cytosolic compartment. Equal volume of lysis buffer without Triton X-114 (20 mM Tris, 150 mM NaCl, pH 7.5) was added to the detergent-rich membrane phase to replace the aqueous supernatant. ¼ volume of Laemmli buffer was added to the cytosolic and membranous phases before analysis by SDS-PAGE gels and western blotting.

Disease monitoring in MRL/lpr mice. Development of nephritis was monitored in MRL/lpr mice by measurement of proteinuria every 2 weeks starting at 4 weeks of age until the end of the study at 14 weeks of age. Urine was collected from the bottom of cages after housing mice in individual cages without bedding for 4 hours. Urine protein was measured by Bradford protein assay (Bio-Rad, catalog #500-006) using 2 μl of urine. Proteinuria and glucosuria were also measured using Chemstrip 10 (Roche, catalog #1 1895362160). In parallel, serum was collected by submandibular bleeding for measurement anti-nuclear auto-antibodies (ANA). To assess for potential treatment toxicities, mice were weighed weekly.

ELISAs for assays antinuclear antibody (ANA) and cytokine production. ANA was measured in 2 μl of serum by ELISA using manufacturer's protocol (Alpha Diagnostics International; catalog # 5210). Results were read on a Biotek Synergy II plate reader equipped with Gen5 software at absorbances of 450 nm and 630 nm, with the 630 nm subtracted from the 450 nm measurement for background reduction.

IFN-γ, IL-10, and IL-17A were measured in 25 μl of serum using BioLegend Max ELISA kit according to the manufacturer's protocols (IFN- γ, catalog #430807; IL-10, catalog #431407; IL-17A, catalog # 432507). Cytokine ELISAs were performed in duplicates averaged for each mouse prior to statistical analysis. Results were read on a Biotek Synergy II plate reader equipped with Gen5 software at absorbance of 450 nm and 570 nm, with the 570 nm subtracted from the 450 nm measurement for background reduction. For ANA and cytokine ELISAs, a standard curve was prepared for each assay and absorbance values were converted into U/mL or pg/mL by linear regression using GraphPad Prism 5.0 software.

Renal pathology. At the time of sacrifice, a kidney was removed from each mouse and transferred into 10% formalin. Samples were paraffin-embedded, sectioned, and stained with Periodic Acid-Schiff (PAS) and hematoxylin. Histology was assessed by scoring for glomerulonephritis (GN), glomerulosclerosis (GS), interstitial nephritis (IN) on a 0-4 scale, as well as determining the percentage of sclerotic and crescentric glomeruli [15;16]. Slides were scored independently by expert pathologists blinded to the treatment groups.

Treatment of mice with Rab geranylgeranyl transferase inhibitor 3-PEHPC and rapamycin. Twenty-four female MRL/lpr mice were separated into four treatment groups: 4 mice were treated with PBS (solvent control for 3-PEHPC), 4 were treated with 0.2% carboxymethylcellulose (CMC, solvent control for rapamycin), 8 were treated with 125 μg/kg 3-

PEHPC in PBS, and 8 were treated with 1 mg/kg rapamycin in CMC. PBS and 3-PEHPC were injected subcutaneously. CMC and rapamycin were injected intraperitoneally in the left lower quadrant of the abdomen 3 times a week. 3-PEHPC was prepared in PBS, filter-sterilized, and stored in aliquots at 4°C until use. Rapamycin solution was prepared freshly on each date by dissolving rapamycin stock solution (prepared in DMSO) in 0.2% CMC warmed to 37°C and mixed thoroughly by vortexing. Rapamycin solution is an emulsion that precipitates out of solution when cooled, so the solution was prepared immediately before injection. Mice were treated for a total of 10 weeks, starting at 4 weeks of age.

Transfection of siRNA. HeLa cells were transfected at 30% confluence in 6-well plates with 200 nM siRNA specific for HRES-1/Rab4 nucleotides 377-399 or scrambled siRNA using the Oligofectamine protocol (Invitrogen/Life Technologies, Gaithersburg, MD). Jurkat cells or primary lymphocytes can only be transfected by siRNA using electroporation, resulting in significant (>50%) loss of viability and altered mitochondrial homeostasis. Therefore, we utilized HeLa cells which can be transfected with siRNA without change in viability using Oligofectamine Transfection Reagent (Invitrogen/Life Technologies). All siRNAs were synthesized with an Alexa-647 tag by Qiagen and delivery regularly exceeding 95% was monitored by flow cytometry. Gene expression was assayed by western blot 48h after transfection.

Statistical analysis. Statistical analyses were performed using Statview 5.0.1 (SAS Institute, Cary, NC) and GraphPad Prism 5.0 Software (San Diego, CA). Data were expressed as the mean ± standard error of the mean (SEM) of individual experiments. Pair-wise repeated measures analysis of variance (ANOVA), two-way ANOVA, and Student's t-tests were used for analysis of results. Changes were considered significant at p value < 0.05.

LEGENDS TO SUPPLEMENTARY FIGURES S1-S7

Fig. S1. Effect of wild-type HRES-1/Rab4 and dominant-negative HRES-1/Rab4^{S27N} (HRES-1/Rab4-DN) on accumulation of mitochondria, detected with MitoTracker Deep Red (MTDR), and on the co-localization of mitochondria with lysosomes, detected with LysoTracker Red (LTR). A, Immunofluorescence microscopy of Jurkat cells carrying doxycycline-inducible GFP-producing control (Control), HRES-1/Rab4 and GFP-producing expression vector (HRES-1/Rab4), or dominant- negative HRES-1/Rab4^{S27N} and GFP-producing expression vector (HRES-1/Rab4-DN) were pre-incubated in the presence (+D) or absence of doxycycline for 24 h and analyzed by confocal microscopy. B, Cumulative analysis of mitochondrial mass (MTDR) lysosomal mass (LTR) and their colocalization using the NIH Image J software. Data represent mean ± SE of 35 to 79 cells per parameter.

Fig. S2. Effect of wild-type HRES-1/Rab4 and dominant-negative HRES-1/Rab4^{S27N} (HRES-1/Rab4-DN) on LC3-I and LC3-II protein levels in Jurkat cells carrying doxycycline-inducible GFP-producing control expression vector (Control), HRES-1/Rab4 and GFP-producing expression vector (HRES-1/Rab4), or dominant-negative HRES-1/Rab4^{S27N} and GFP-producing expression vector (HRES-1/Rab4-DN). A, Endogenous LC3 was assessed by western blot analysis in cells cultured in the presence of 200 nM bafilomycin A1, in the presence (+D) or absence of doxycycline, without or with 50 nM rapamycin for 24 h. Cumulative data represent 4 independent experiments. B, Processing of exogenous LC3 was assessed 48 h after infection with AAV expressing FP650-LC3 fusion protein. Cells were cultured in the presence or absence of 200 nM Bafi for 24 h before extracting protein lysates for western blot analysis. Representative western blot (top panel) and cumulative analysis of 4 independent experiments (bottom panel) are shown. p values < 0.05 reflect two-tailed paired t-tests.

Fig. S3. Increased expression of Rab4A and depletion of Drp1 in lupus-prone mice. A, Western blot analysis of Rab4A expression in 4-week-old lupus-prone NZB x NZW F1 (NZB/W F1) female mice in comparison to age-matched NZW/LacJ (NZW) and C57BL/6 (B6) female controls. Protein lysates were prepared from un-fractionated splenocytes, T cells, macrophages, or thymocytes, as indicated. 4-month-old (4M) disease-free NZB/W F1 and B6.NZMSle1.Sle2.Sle3 were also analyzed. Data represent mean ± SE of 6-8 mice per strain. B, Western blot analysis of Rab5 expression in 4-week-old NZB/W F1 female mice in comparison to age-matched NZW and B6 female controls as well as in 4-month-old (4M) NZB/W F1 and B6 controls. C, Western blot analysis of CD3ζ and CD4 protein levels in 4-week-old and 4-month-old (4M) NZB/W F1 as well as NZW and B6 control mice. D, Western blot analysis of Beclin 1 in 4-week-old NZB/W F1 as well as NZW and B6 control mice. E, NO production in splenocyte subsets of 4-week-old NZB/W F1 lupus-prone mice as well as age-matched NZW and B6 control mice. NO was measured by DAF-FM fluorescence using flow cytometry and expressed as mean fluorescence intensity (MFI) relative to B6 control mice normalized to 1.0 for each cell type. Data represent mean ± SE in 8 mice per strain. p values reflect comparison to B6 controls.

Fig. S4. Assessment of mTOR activity via phosphorylation and expression of its substrates S6K and 4E-BP1 in 4-week-old female NZB/NZW F1 mice and NZW as well as B6 control mice. mTOR activity was also evaluated in 4-month-old (4M) and 6-month-old NZB/NZW F1 mice

(6M) relative to 4-month-old B6 mice. For each parameter 4 or more mice were analyzed; p values < 0.05 are indicated.

Fig. S5. Effect of aging on mitochondrial homeostasis evaluated by NO production (DAF-FM fluorescence), mitochondrial transmembrane potential ($\Delta\Psi_m$, $DiOC_6$ and TMRM fluorescence), and mitochondrial mass (MTG fluorescence) in mouse splenocytes using flow cytometry. A, Assessment of aging on mitochondrial homeostasis in B6 mice at ages of 3 months (B6 3M), 8 months (B6 8M) and 12 months (B6 12M). Data represent mean ± SE in 4-8 mice per group. p values < 0.05 are indicated. B, 6-month-old (NZB/W F1 6M) and 11-month-old NZB/W F1 lupus prone mice (NZB/W F1 11M) were evaluated relative to 6-month-old NZW controls (NZW 6M). C, Western blot detection of VDAC relative to β-actin in splenocytes of 6-month-old NZB/W F1 lupus prone mice (NZB/W F1) and age-matched B6 and NZW controls. Bar charts reflect cumulative analysis of 4-6 mice per group; $p < 0.05$ is indicated.

Fig. S6. Influence of 3-PEHPC on partitioning of HRES-1/Rab4 and Rab5 to the cytosol. Jurkat cells were incubated without or with 0.5 mM or 2.0 mM 3-PEHPC for 24 h. HRES-1/Rab4 and Rab5 protein levels relative to β-actin were analyzed by western blot of cytosolic and membrane fractions. Representative western blot (left) and mean ± SE two independent experiments are shown (right panel).

Fig. S7. Schematic model for inhibition of mitophagy and accumulation of mitochondria in lupus T cells. A, Regulation of autophagy and mTOR pathways by HRES-1/Rab4. Overall stimulation of autophagy by HRES-1/Rab4 is indicated by the enhanced lipidation of LC3, resulting in lysosomal degradation of CD4, CD3ζ, and Drp1. In the absence of Drp1, mitophagy is inhibited, resulting in the accumulation of mitochondria. B, Molecular hierarchy of metabolic checkpoints that control increased T-cell activation through the accumulation of mitochondria and reorganization of the supramolecular activating complex (SMAC) in SLE. NO induces expression of HRES-1/Rab4 and positive feedback amplification of mTORC1, causing 1) mTORC1-dependent (rapamycin-inhibited) enhancement of recycling and degradation of CD3ζ and CD4 and 2) mTORC1-independent (rapamycin-resistant) but Rab geranylgeranyl transferase-dependent (3-PEHPC-inhibited) degradation of Drp1 and accumulation of mitochondria. Color coding, blue: molecules; green: pathways.

REFERENCES

(1) Tan EM, Cohen AS, Fries JF, Masi AT, McShane DJ, Rothfield NF et al. The 1982 revised criteria for the classification of systemic lupus erythematosus. Arth Rheum 1982; 25:1271-1277.

(2) Hochberg MC. Updating the American College of Rheumatology revised criteria for the classification of systemic lupus erythematosus. Arth Rheum 1997; 40(9):1725.

(3) Bombardier C, Gladman DD, Urowitz MB, Caron D, Chang CH, the committee on prognosis studies in SLE. Derivation of the SLEDAI. A disease activity index for lupus patients. Arth Rheum 1992; 35:630-640.

(4) Perl A, Gonzalez-Cabello R, Lang I, Gergely P. Effector activity of OKT4+ and OKT8+ T-cell subsets in lectin- dependent cell-mediated cytotoxicity against adherent HEp-2 cells. Cell Immunol 1984; 84:185-193.

(5) Ishihara N, Nomura M, Jofuku A, Kato H, Suzuki SO, Masuda K et al. Mitochondrial fission factor Drp1 is essential for embryonic development and synapse formation in mice. Nat Cell Biol 2009; 11(8):958-966.

(6) Banki K, Hutter E, Gonchoroff N, Perl A. Elevation of mitochondrial transmembrane potential and reactive oxygen intermediate levels are early events and occur independently from activation of caspases in Fas signaling. J Immunol 1999; 162:1466-1479.

(7) Nagy G, Koncz A, Perl A. T cell activation-induced mitochondrial hyperpolarization is mediated by Ca^{2+}- and redox-dependent production of nitric oxide . J Immunol 2003; 171:5188-5197.

(8) Perl A, Hanczko R, Doherty E. Assessment of mitochondrial dysfunction in lymphocytes of patients with systemic lupus erythematosus. In: Perl A, editor. Meth. Mol.Med. Autoimmunity: Methods and Protocols. 2 ed. Clifton,NJ: Springer; 2012. 61-89.

(9) Hanczko R, Fernandez D, Doherty E, Qian Y, Vas Gy, Niland B et al. Prevention of hepatocarcinogenesis and acetaminophen-induced liver failure in transaldolase-deficient mice by N-acetylcysteine. J Clin Invest 2009; 119:1546-1557.

(10) Fernandez DR, Telarico T, Bonilla E, Li Q, Banerjee S, Middleton FA et al. Activation of mTOR controls the loss of TCRζ in lupus T cells through HRES-1/Rab4-regulated lysosomal degradation. J Immunol 2009; 182:2063-2073.

(11) Saeed AI, Sharov V, White J, Li J, Liang W, Bhagabati N et al. TM4: A free, open-source system for microarray data management and analysis. Biotechniques 2003; 34(2):374-378.

(12) Nagy G, Ward J, Mosser DD, Koncz A, Gergely P, Stancato C et al. Regulation of CD4 Expression via Recycling by HRES-1/RAB4 Controls Susceptibility to HIV Infection. J Biol Chem 2006; 281:34574-34591.

(13) Rubinsztein DC, Cuervo AM, Ravikumar B, Sarkar S, Korolchuk VI, Kaushik S et al. In search of an autophagomometer. Autophagy 2009; 5(5):585-589.

(14) Baron RA, Tavare R, Figueiredo AC, Blazewska KM, Kashemirov BA, McKenna CE et al. Phosphonocarboxylates inhibit the second geranylgeranyl addition by Rab geranylgeranyl transferase. J Biol Chem 2009; 284(11):6861-6868.

(15) Passwell J, Schreiner GF, Nonaka M, Beuscher HU, Colten HR. Local extrahepatic expression of complement genes C3, factor B, C2, and C4 is increased in murine lupus nephritis. J Clin Invest 1988; 82(5):1676-1684.

(16) Bao L, Haas M, Pippin J, Wang Y, Miwa T, Chang A et al. Focal and segmental glomerulosclerosis induced in mice lacking decay-accelerating factor in T cells. J Clin Invest 2009; 119(5):1264-1274.

Figure S1

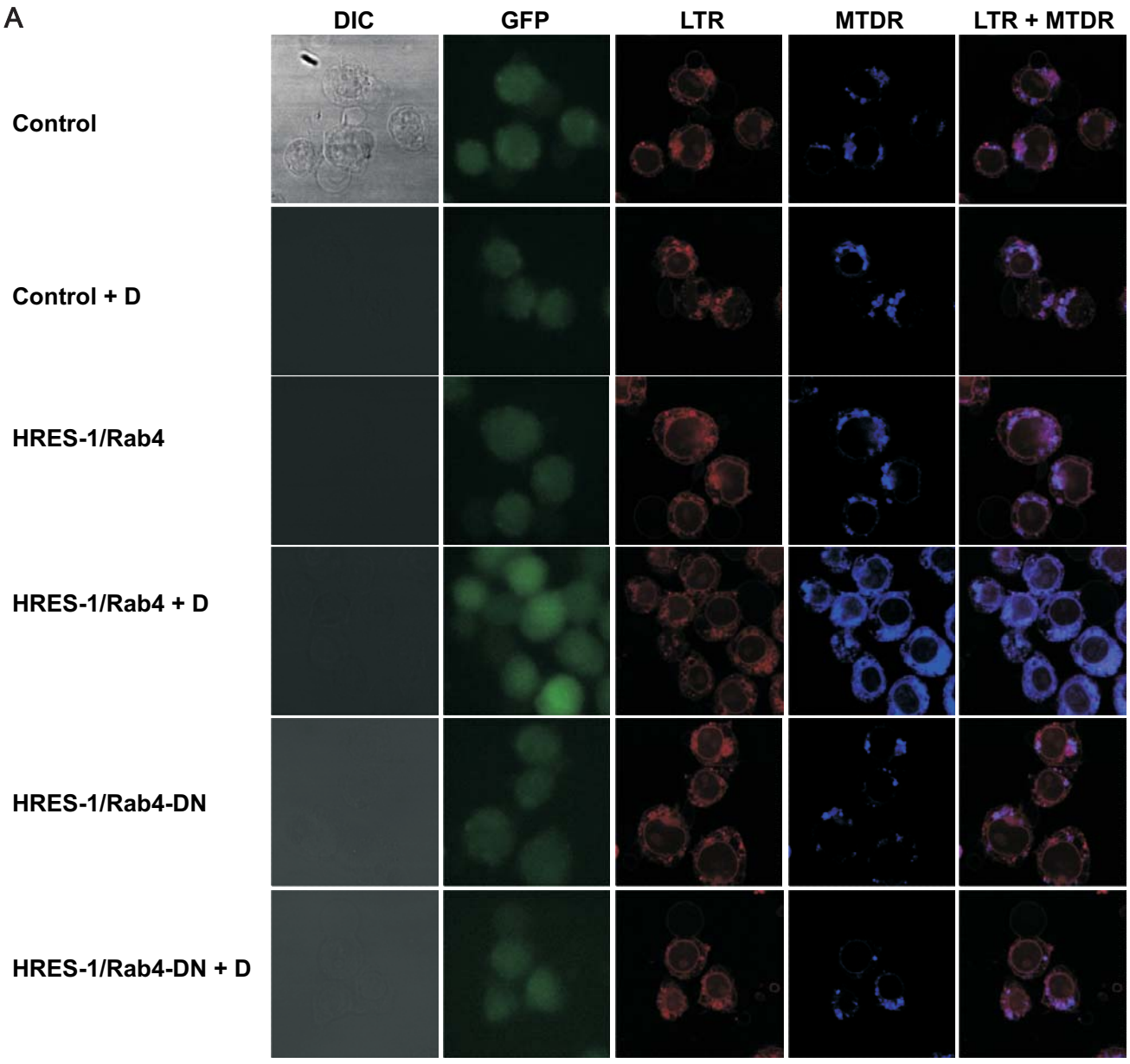
A
DIC
GFP
LTR
MTDR
LTR + MTDR
Control
Control + D
HRES-1/Rab4
HRES-1/Rab4 + D
HRES-1/Rab4-DN
HRES-1/Rab4-DN + D

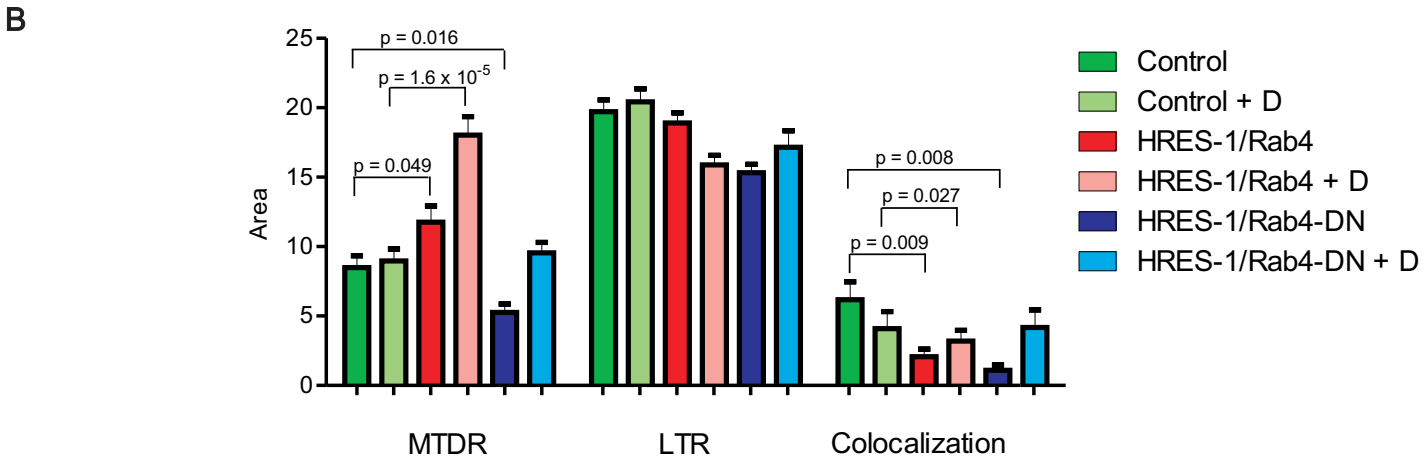
B
Area
25
20
15
10
5
0
p = 0.016
p = 1.6 x 10-5
p = 0.049
p = 0.008
p = 0.027
p = 0.009
MTDR
LTR
Colocalization
Control
Control + D
HRES-1/Rab4
HRES-1/Rab4 + D
HRES-1/Rab4-DN
HRES-1/Rab4-DN + D

Figure S2

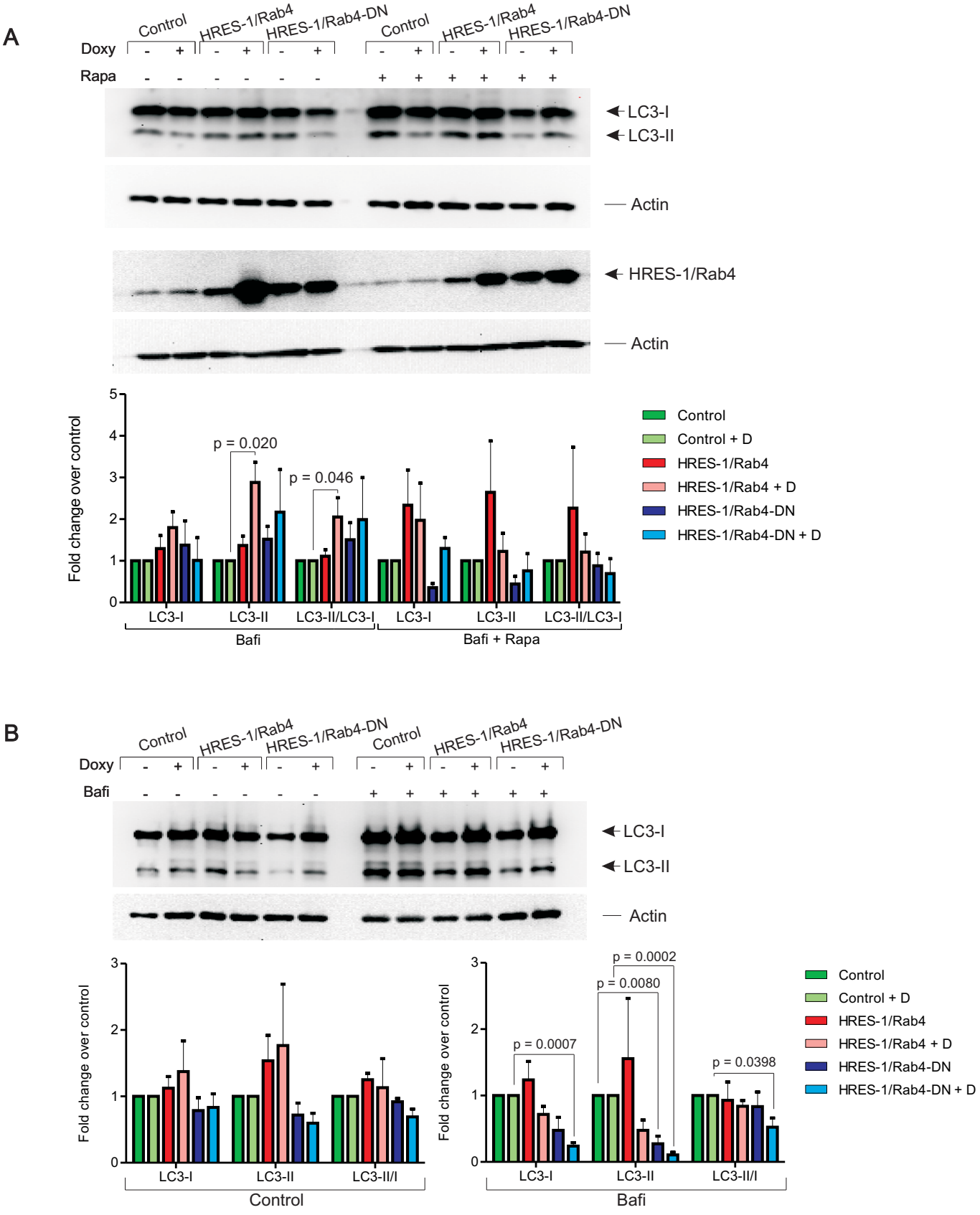
A
Control
HRES-1/Rab4
HRES-1/Rab4-DN
Control
HRES-1/Rab4
HRES-1/Rab4-DN
Doxy
Rapa
LC3-I
LC3-II
Actin
HRES-1/Rab4
Actin
Fold change over control
p = 0.020
p = 0.046
Control
Control + D
HRES-1/Rab4
HRES-1/Rab4 + D
HRES-1/Rab4-DN
HRES-1/Rab4-DN + D
LC3-I
LC3-II
LC3-II/LC3-I
Bafi
Bafi + Rapa
B
Control
HRES-1/Rab4
HRES-1/Rab4-DN
Control
HRES-1/Rab4
HRES-1/Rab4-DN
Doxy
Bafi
LC3-I
LC3-II
Actin
Fold change over control
p = 0.0007
p = 0.0080
p = 0.0002
p = 0.0398
Control
Control + D
HRES-1/Rab4
HRES-1/Rab4 + D
HRES-1/Rab4-DN
HRES-1/Rab4-DN + D
LC3-I
LC3-II
LC3-II/I
Control
Bafi

Figure S3

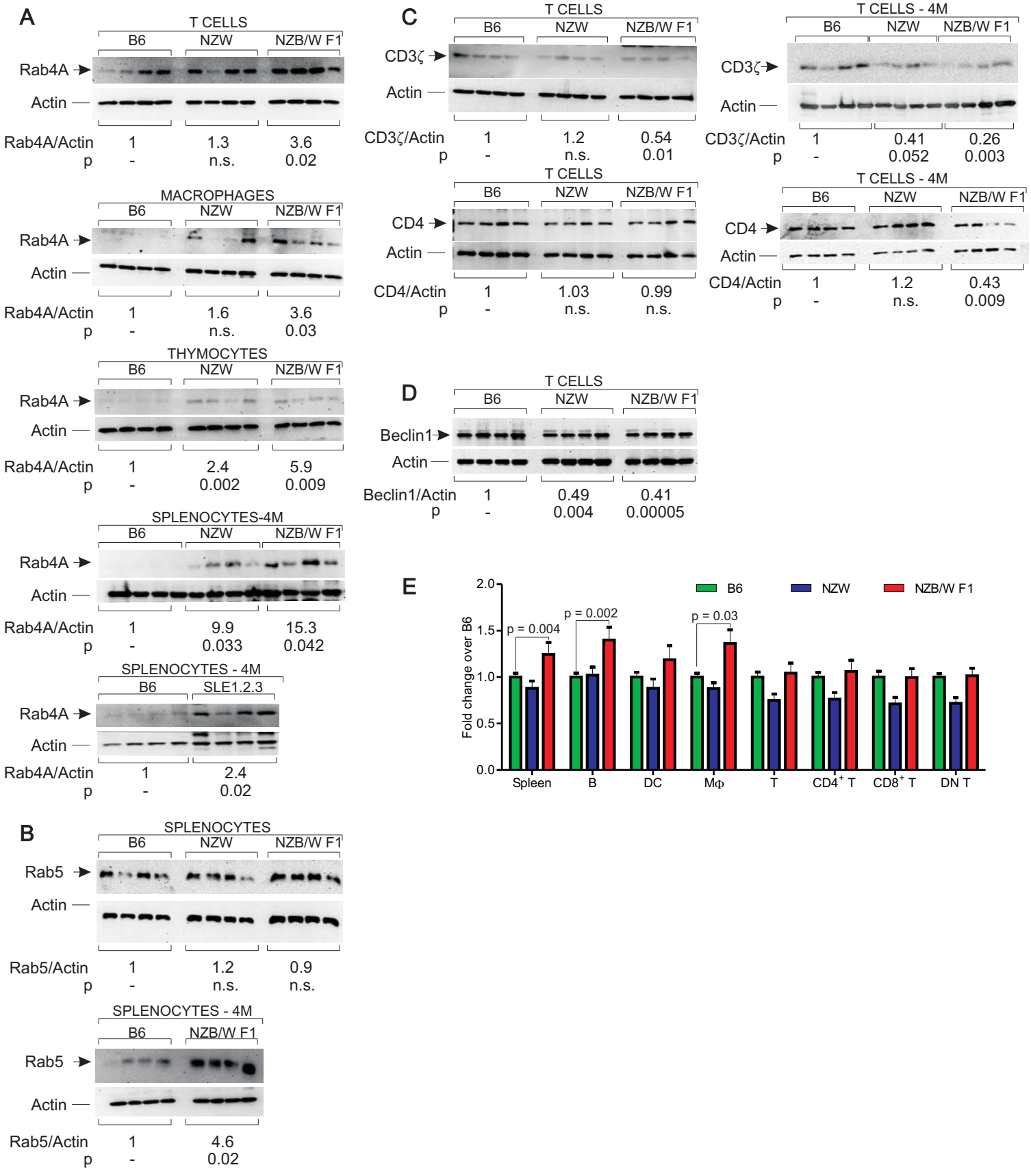
A
T CELLS
B6
NZW
NZB/W F1
Rab4A
Actin
Rab4A/Actin 1 1.3 3.6
p - n.s. 0.02
MACROPHAGES
Rab4A/Actin 1 1.6 3.6
p - n.s. 0.03
THYMOCYTES
Rab4A/Actin 1 2.4 5.9
p - 0.002 0.009
SPLENOCYTES-4M
Rab4A/Actin 1 9.9 15.3
p - 0.033 0.042
SPLENOCYTES - 4M
SLE1.2.3
Rab4A/Actin 1 2.4
p - 0.02
B
SPLENOCYTES
Rab5
Rab5/Actin 1 1.2 0.9
p - n.s. n.s.
SPLENOCYTES - 4M
Rab5/Actin 1 4.6
p - 0.02
C
T CELLS
CD3ζ
CD3ζ/Actin 1 1.2 0.54
p - n.s. 0.01
T CELLS - 4M
CD3ζ/Actin 1 0.41 0.26
p - 0.052 0.003
CD4
CD4/Actin 1 1.03 0.99
p - n.s. n.s.
CD4/Actin 1 1.2 0.43
p - n.s. 0.009
D
Beclin1
Beclin1/Actin 1 0.49 0.41
p - 0.004 0.00005
E
Fold change over B6
p = 0.004
p = 0.002
p = 0.03
Spleen
B
DC
MΦ
T
CD4+ T
CD8+ T
DN T

Figure S4

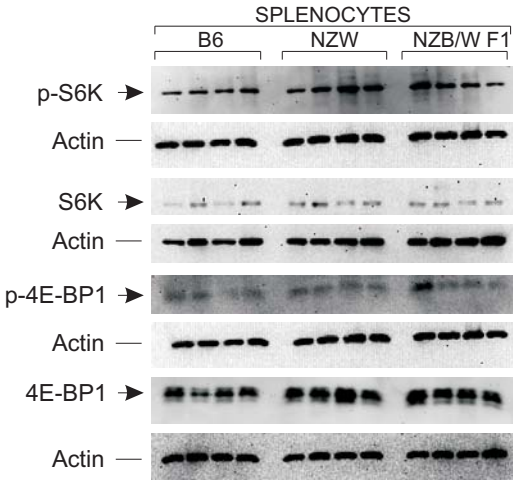
SPLENOCYTES
B6
NZW
NZB/W F1
p-S6K
Actin
S6K
Actin
p-4E-BP1
Actin
4E-BP1
Actin

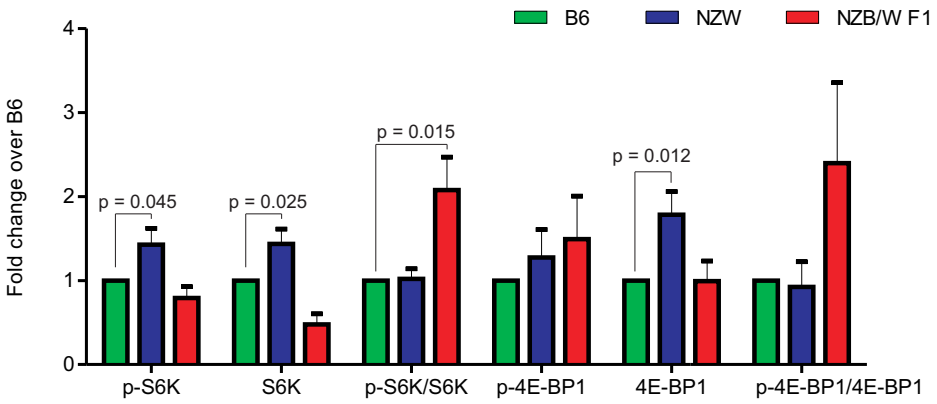
B6
NZW
NZB/W F1
Fold change over B6
p = 0.045
p = 0.025
p = 0.015
p = 0.012
p-S6K
S6K
p-S6K/S6K
p-4E-BP1
4E-BP1
p-4E-BP1/4E-BP1

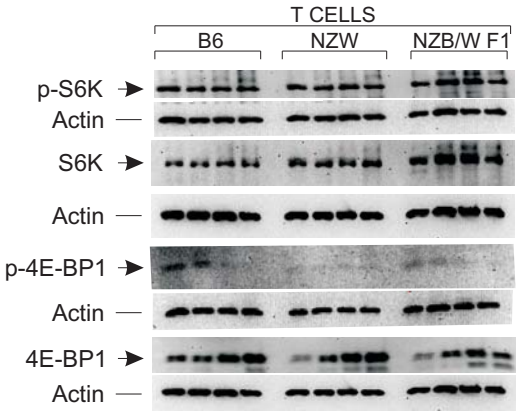
T CELLS
B6
NZW
NZB/W F1
p-S6K
Actin
S6K
Actin
p-4E-BP1
Actin
4E-BP1
Actin

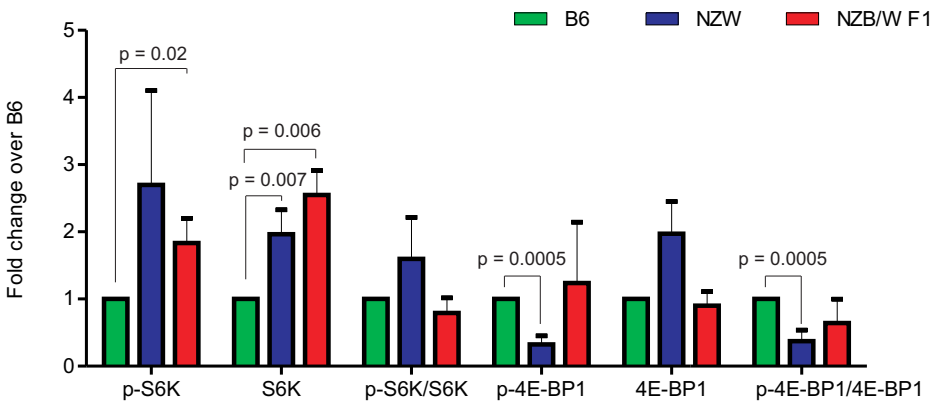
B6
NZW
NZB/W F1
Fold change over B6
p = 0.02
p = 0.006
p = 0.007
p = 0.0005
p = 0.0005
p-S6K
S6K
p-S6K/S6K
p-4E-BP1
4E-BP1
p-4E-BP1/4E-BP1

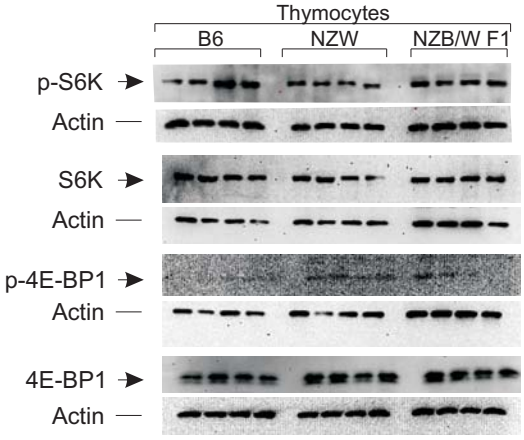
Thymocytes
B6
NZW
NZB/W F1
p-S6K
Actin
S6K
Actin
p-4E-BP1
Actin
4E-BP1
Actin

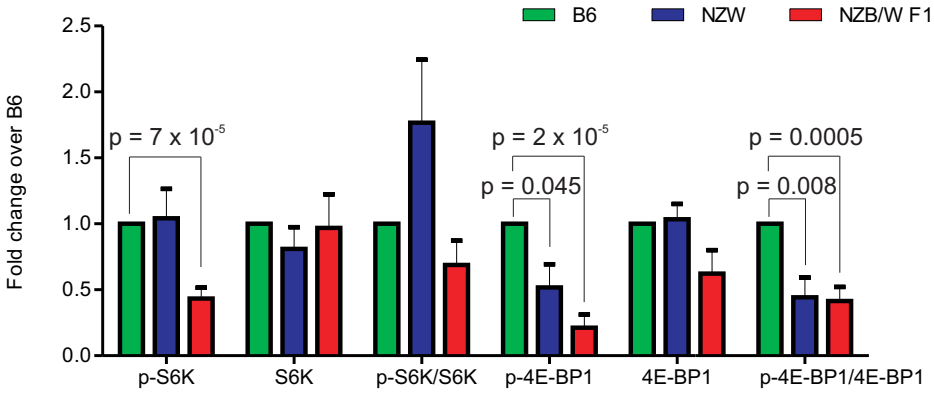
B6
NZW
NZB/W F1
Fold change over B6
p = 7 x 10-5
p = 2 x 10-5
p = 0.0005
p = 0.045
p = 0.008
p-S6K
S6K
p-S6K/S6K
p-4E-BP1
4E-BP1
p-4E-BP1/4E-BP1

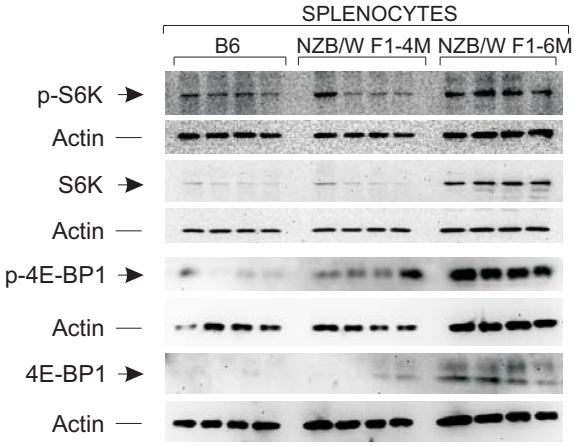
SPLENOCYTES
B6
NZB/W F1-4M
NZB/W F1-6M
p-S6K
Actin
S6K
Actin
p-4E-BP1
Actin
4E-BP1
Actin

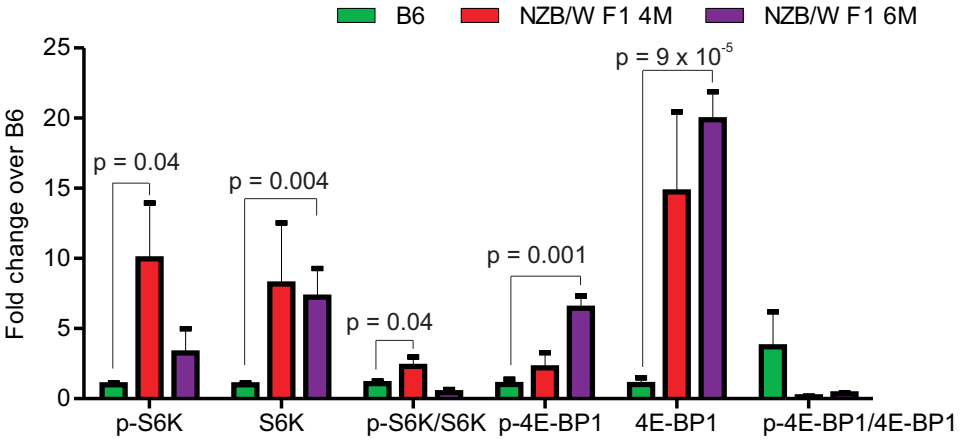
B6
NZB/W F1 4M
NZB/W F1 6M
Fold change over B6
p = 0.04
p = 0.004
p = 0.04
p = 0.001
p = 9 x 10-5
p-S6K
S6K
p-S6K/S6K
p-4E-BP1
4E-BP1
p-4E-BP1/4E-BP1

Figure S5

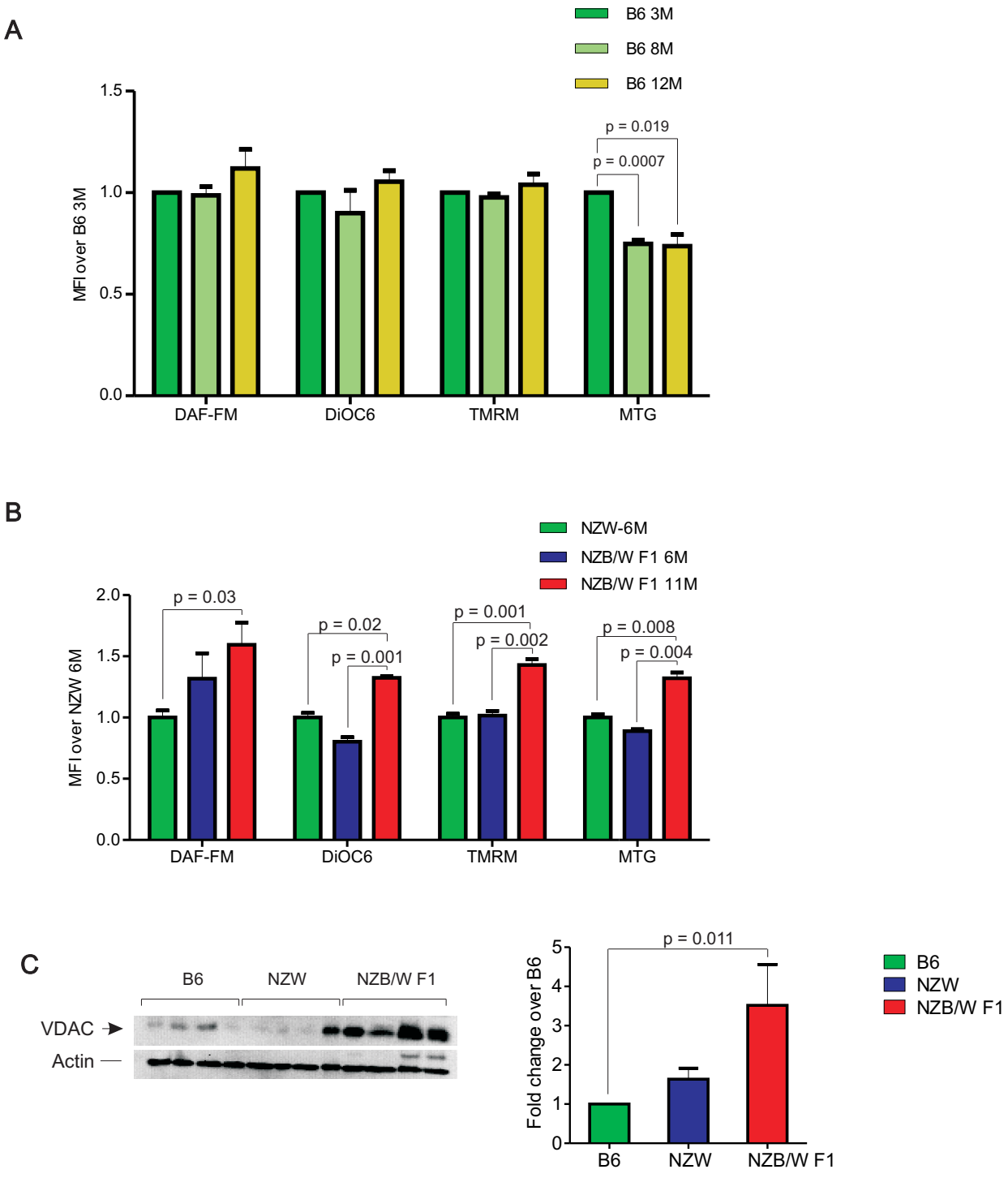
A
B6 3M
B6 8M
B6 12M
MFI over B6 3M
1.5
1.0
0.5
0.0
p = 0.019
p = 0.0007
DAF-FM
DiOC6
TMRM
MTG
B
NZW-6M
NZB/W F1 6M
NZB/W F1 11M
MFI over NZW 6M
2.0
1.5
1.0
0.5
0.0
p = 0.03
p = 0.02
p = 0.001
p = 0.001
p = 0.002
p = 0.008
p = 0.004
DAF-FM
DiOC6
TMRM
MTG
C
B6
NZW
NZB/W F1
VDAC
Actin
p = 0.011
Fold change over B6
5
4
3
2
1
0
B6
NZW
NZB/W F1
B6
NZW
NZB/W F1

Figure S6

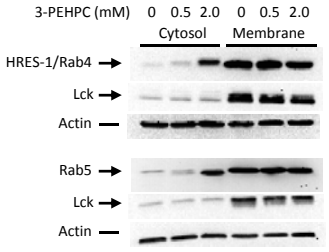
3-PEHPC (mM) 0 0.5 2.0 0 0.5 2.0
Cytosol
Membrane
HRES-1/Rab4
Lck
Actin
Rab5
Lck
Actin

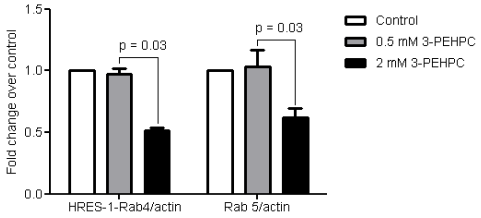
Fold change over control
1.5
1.0
0.5
0.0
p = 0.03
p = 0.03
HRES-1-Rab4/actin
Rab 5/actin
Control
0.5 mM 3-PEHPC
2 mM 3-PEHPC

Figure S7

A

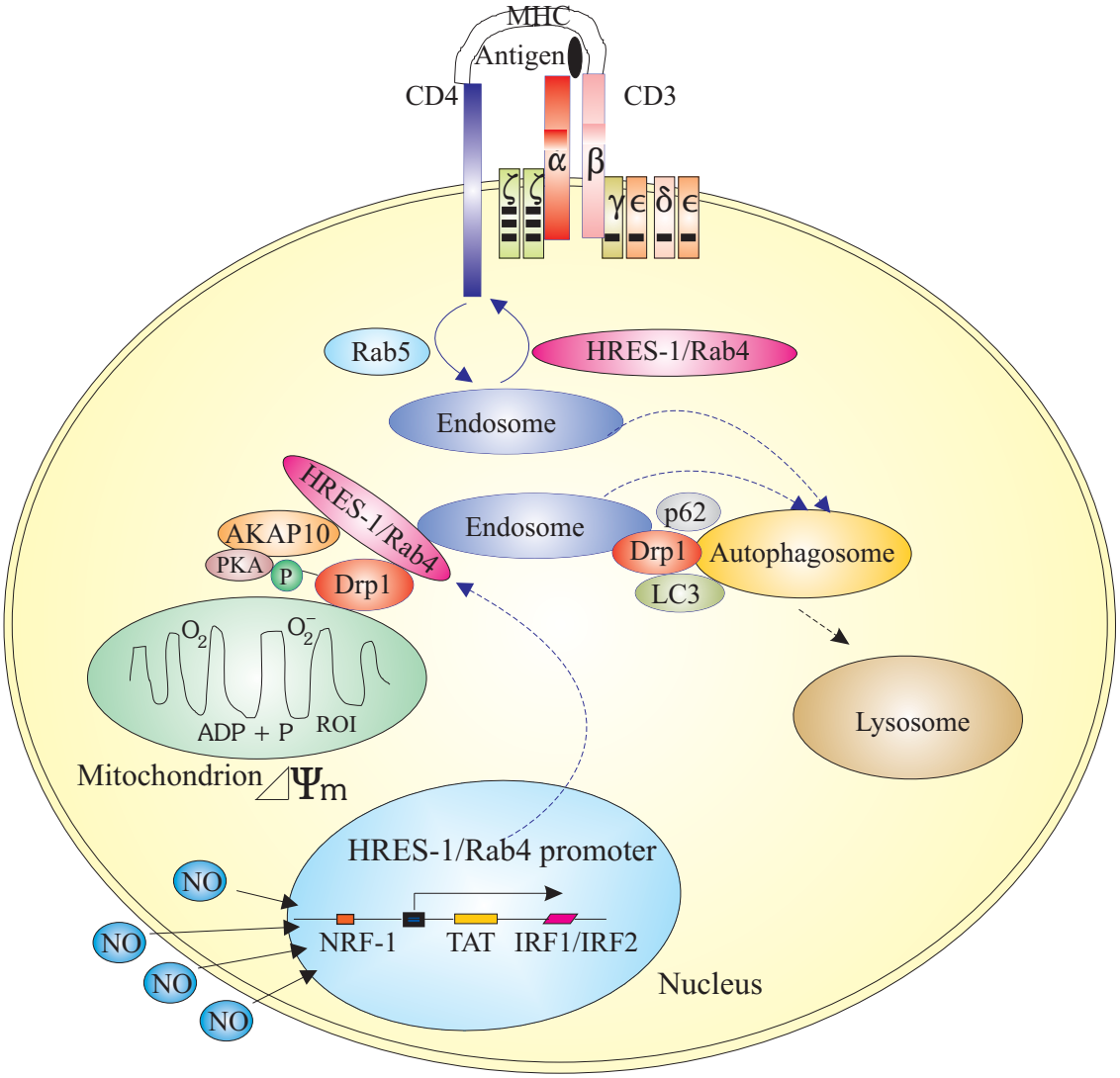
MHC
Antigen
CD4
CD3
α
β
ζ
ζ
γ
ϵ
δ
ϵ
Rab5
HRES-1/Rab4
Endosome
HRES-1/Rab4
AKAP10
PKA
P
Drp1
Endosome
p62
Drp1
Autophagosome
LC3
Lysosome
O2
O2−
ADP + P
ROI
Mitochondrion ΔΨm
HRES-1/Rab4 promoter
NO
NO
NO
NO
NRF-1
TAT
IRF1/IRF2
Nucleus

B

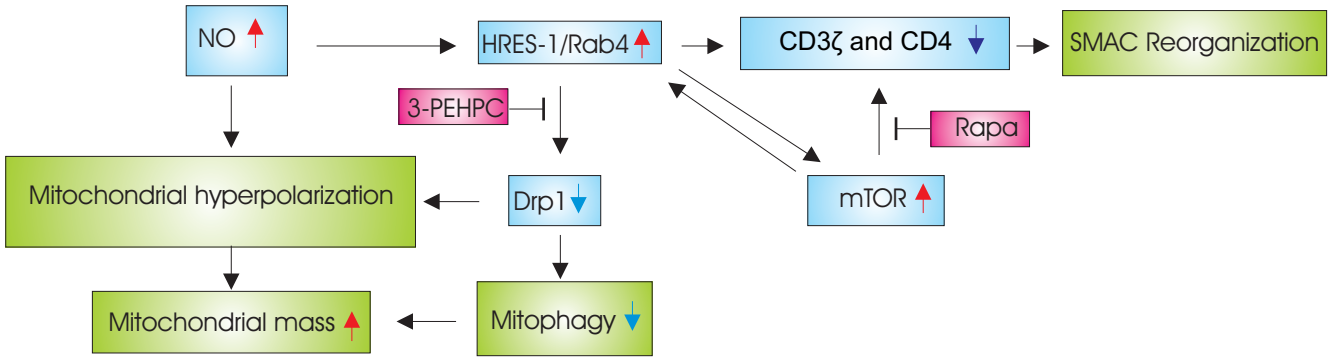
NO
HRES-1/Rab4
CD3ζ and CD4
SMAC Reorganization
3-PEHPC
Rapa
Mitochondrial hyperpolarization
Drp1
mTOR
Mitochondrial mass
Mitophagy